

SUPPORTING INFORMATION

1D polymeric Pt cyanoximate: a strategy toward luminescence in the near-infrared region beyond 1000 nm

Danielle R. Klaus,¹ Matthew Keene,¹ Svitlana Silchenko,² Mikhail Berezin,^{3*}
and Nikolay Gerasimchuk^{1*}

Contents

1D polymeric Pt cyanoximate: a strategy toward luminescence in the near-infrared region beyond 1000 nm	0
1. Thermodynamic and optical properties of the complexes and ligands in solutions....	3
1.1. The pK _a determination of the new cyanoxime ligand 1	3
1.2. Some thermodynamic and geometrical parameters of a series of amide-cyanoximes and their complexes	4
1.3. Electrical conductivity of complexes	6
2. Crystal structures	7
2.1. The cyanoxime HDECO (compound 1)	7
2.2. Crystal data for yellow monomeric Pt(DECO) ₂ (complex 3)	8
2.2.1. Crystal packing in the structure of yellow monomeric Pt(DECO) ₂ , (complex 3)	9
2.2.2. Geometrical features of the cyanoxime anion DECO ⁻ in yellow monomeric Pt(DECO) ₂ (complex 3).	10
2.3. Crystal data for the red dimer Pt(DECO) ₂ (complex 4).	11
2.3.1. Geometry of cyanoxime anions DECO ⁻ in the structure of red dimeric Pt(DECO) ₂ (complex 4).	12
2.3.2. Perspective views of the unit cell content of the red dimer Pt(DECO) ₂ (4)	13
2.3.3. Crystal packing in the structure of red dimeric Pt(DECO) ₂ (complex 4) in detail... ..	14
2.4. Crystal data for monomeric yellow Pd(DECO) ₂ (complex 6)	15

2.4.1	Structure and numbering scheme for Pd(DECO) ₂ (complex 6).....	16
2.4.2	Geometry of the cyanoxime anion DECO ⁻ in Pd complex 6	17
2.4.3	Simulated powder XRD patterns for Pt(DECO) ₂ , yellow monomer (3), and yellow Pd(DECO) ₂ complex (6).	18
2.5	Crystal data for all studied compounds: H(DECO)(1) and its complexes 3, 4, 6	19,20
2.6	Selected values of bond lengths and valence angles	21
3	Microscopy images of crystals of studied complexes	25
3.4	Samples of known and established 1D coordination Pt-polymers	25
3.5	Optical microscopy images of crystals in Pt - DECO system.....	26
3.6	Optical microscope images of all three polymorphs of Pt(DECO) ₂	27
3.7	Optical microscope images of polymeric Pt(DECO) ₂	28
3.8	Scanning Electron Microscopy images of 1D polymer.....	29
4	Synthesis (additional information)	32
4.4	HDECO (compound 1).....	32
4.5	Synthesis of [Pt(DECO) ₂] _n (5) under air-free conditions.....	33
4.6	Stability of polymeric Pt-cyanoximate 5 in the presence of DMSO.....	34
5	Hardware for spectroscopy measurements	35
5.4	Tablet / pellet holder for spectroscopy measurements	35
5.5	Variable temperature photoluminescence measurements instrument design	36
5.6	Handling of samples for variable temperature photoluminescence measurements.	37
5.7	Solid state absorption spectra of tablets.....	38
6	Optical and spectroscopic properties of the complexes	39
6.1	Scattering properties of polymeric Pt-cyanoximate 5	39
6.2	Kinetics of the particles growth in solution of dark-green 1D polymeric complex 5	40
6.3	Particles size measurements for the polymeric complex 5 in aqueous solutions of Na-decanoate micelles	41
6.4	UV-Vis spectroscopy measurements (summary)	43

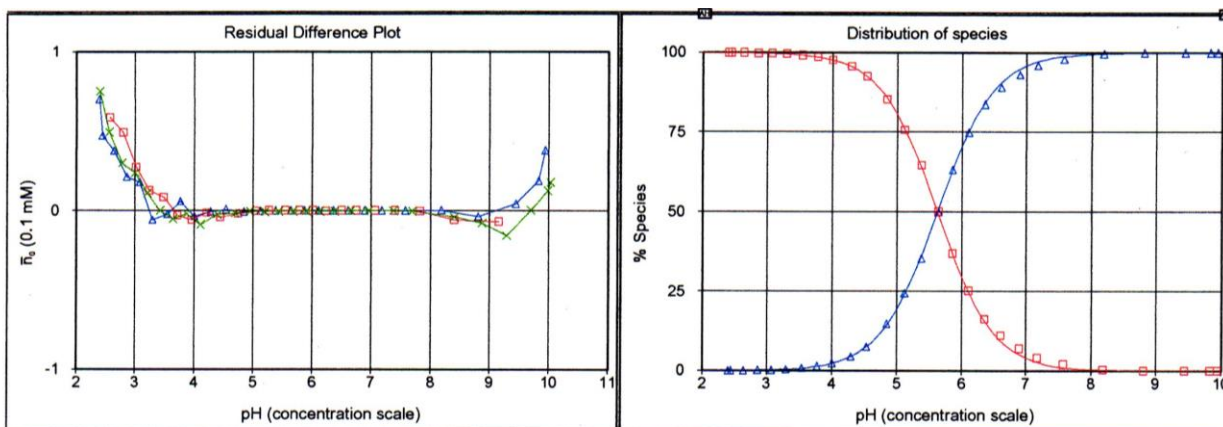
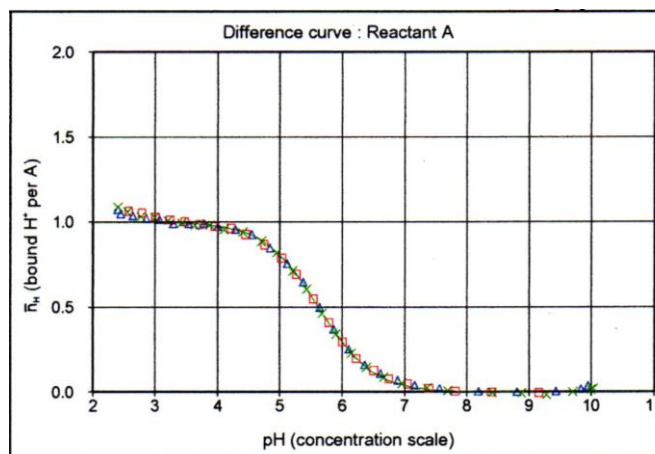
6.5	Solid state absorption spectra recorded as fine suspensions in mineral oil	44
6.6	Solid state absorption spectra of tablets.....	45
6.7	EPR spectra of solid samples of 1D polymer 5	46
6.8	Photoluminescence of powder samples	47
6.9	Effect air on photoluminescence of complex 5	49
6.10	Absolute quantum yield determination.....	49
6.11	Temperature dependence of the emission line width for solid sample of dark-green polymeric complex 5	51
6.12	The emission line shape analysis for solid sample of complex 5 (in KBr pellet; at 5% concentration) at -165°C.	52
6.13	The emission line shape analysis for complex 5 at +50°C.....	53
6.14	The emission spectra of other two dark-green polymeric Pt-cyanoximates.....	53
6.15	The absorption and emission spectra of POCP.....	54
6.16	The absorption and emission spectra of MGS.....	55
6.17	Oxidation of 1D-polymeric complex 5 with elemental Br ₂	56,57
6.18	Redox flexibility of oxime/nitroso compounds.....	58

1. Thermodynamic and optical properties of the complexes and ligands in solutions.

1.1. The pK_a determination of the new cyanoxime ligand **1**

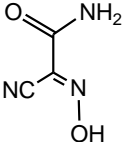
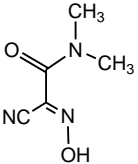
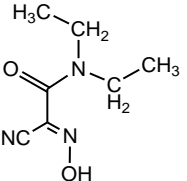
Experimental details of potentiometric determination of pK_a for studied ligand HDECO, **1**, $\text{NC}(\text{N}=\text{O}-\text{H})-\text{C}(\text{O})\text{N}(\text{C}_2\text{H}_5)_2$.

Titration curve:



The titration was performed three times at 23°C in the isopropyl alcohol (ISA) water mixture. The weighed amount of compound **1**, H(DECO), (3.08 mg) was placed into a titration vial. Sixteen milliliters of ISA water was delivered automatically to the vial. The pH of the solution was adjusted to 10 by adding 0.5 M KOH automatically. The titration with 0.5M HCl was performed automatically until a pH value of 2.5 was reached. To perform the second and third titrations, an additional volume of ISA water (1 mL and 1 mL) was delivered automatically to the titration vial, respectively. The datasets for the three titrations were combined in the RefinementPro program to create a Multiset for pK_a calculation. Also, these datasets were combined and extrapolated to a zero ISA concentration.

1.2. Some thermodynamic and geometrical parameters of a series of amide-cyanoximes and their complexes

Compound	<i>pH</i> titration pK _a	¹ H NMR data			X-ray data of bonds length, Å			Ref.
		T _c , °C	k _c , s ⁻¹	ΔG [‡] , kJ/M	amide group N3-C3	nitroso/oxime group N1-O1	O1-H	
H(ACO) 	5.034±0.002	50	72	67.7±0.06	1.331	1.355	1.01	[1,2]
H(DCO) 	5.52±0.03	80	126	72.6±0.07	1.328	1.360	0.96	[1,3]
H(DECO), 1 	5.622±0.005	60	60	70.5±0.09	1.321	1.372	0.92	this work
Pd(DECO)₂, 3 yellow, monomeric	-	55	159	66.8±1	1.323, 1.326 ^a	1.247, 1.247 ^a	-	this work
Pt(DECO)₂, 6 yellow, monomeric	-	100	146	76.6±1	1.321, 1.325 ^a	1.249, 1.249 ^a	-	this work

^a – two slightly different ligands formed two chelate rings in the structures

Citations from the Table S4:

1. K.V. Domasevitch, N.N. Gerasimchuk, A.A. Mokhir. "Organoantimony(V) cyanoximates: synthesis, spectra and crystal structures." *Inorganic Chemistry*. **2000**, 39 (6), 1227- 1237.
2. Gerasimchuk, N.; Esaulenko, A.N.; Dalley, K.N.; Moore, C. "2-Cyano-2-isonitroso acetamide and its Ag(I) complexes. Silver(I) cyanoximate as a non-electric gas sensor." *Dalton Transactions*, **2010**, 39, 749-764.
3. Yu.A. Simonov, A.A. Dvorkin, N.N. Gerasimchuk, K.V. Domasevitch, T.I. Malinovskii. "Crystal structure of a new cyanoxime - 2-Nitroso-2-cyan-N,N-dimethylacetamide." *Kristallografiya*. **1990**, 35 (3), 766-768.

1.3. *Electrical conductivity of complexes*

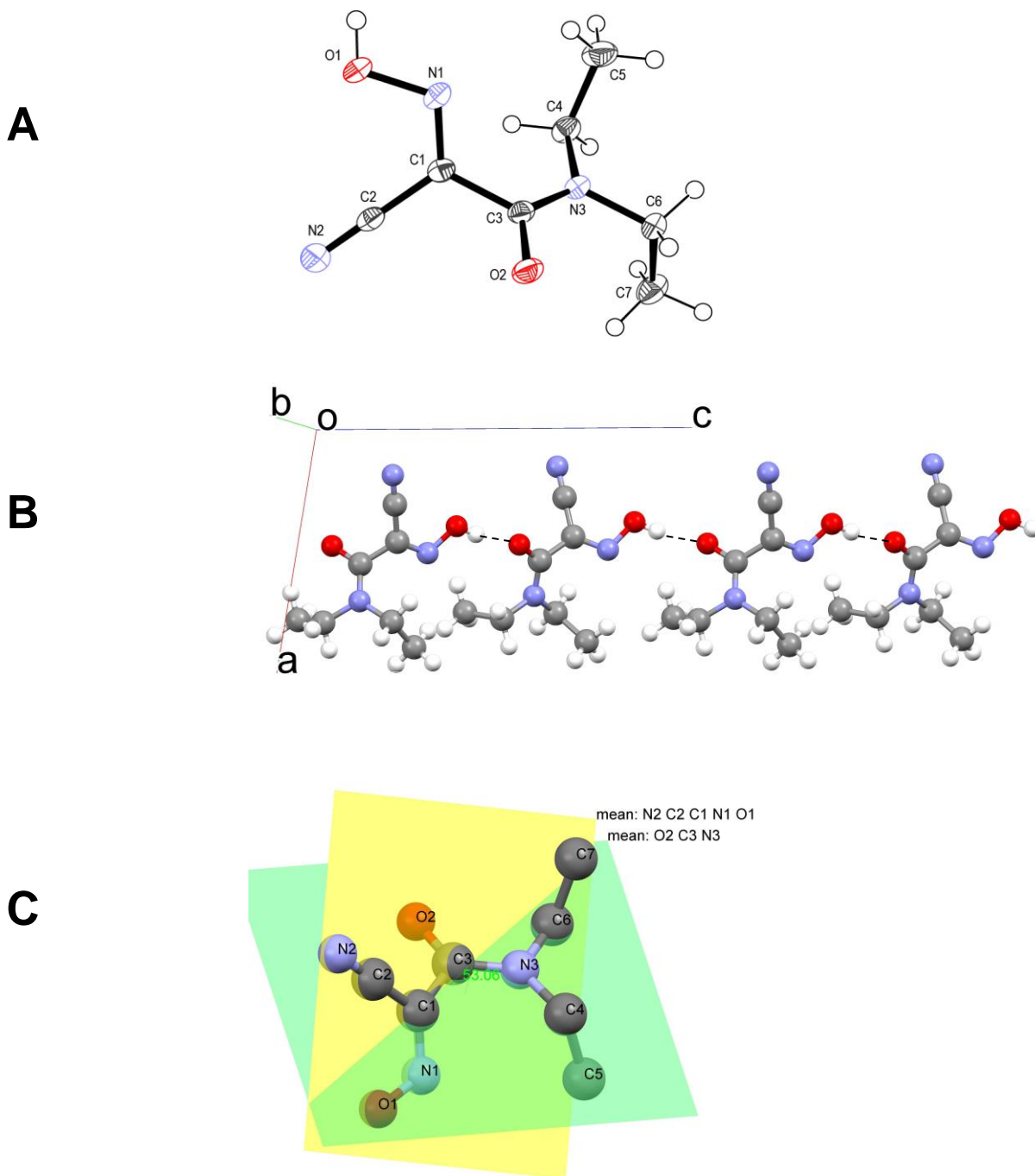
Electrical conductivity measurements were carried out at 22°C in DMSO solutions at 1 mM concentrations of synthesized Pd, Pt-complexes, using the Vernier LabQuest Digital Conductivity meter. An electrode was calibrated with 1 mM DMSO solutions of $\text{N}(\text{C}_4\text{H}_9)_4^+\text{Br}^-$, $\text{P}(\text{C}_6\text{H}_5)_4^+\text{Br}^-$ and K_2PtCl_4 . The values of the conductivities are listed here in the table **S1** below.

Compound:	Conductivity, $\mu\text{S}/\text{cm}$	Electrolyte type
Pure DMSO	2.5	no conductance
$\text{N}(\text{C}_4\text{H}_9)_4\text{Br}$	26.5	1 : 1
$\text{P}(\text{C}_6\text{H}_5)\text{Br}$	26.1	1 : 1
K_2PtCl_4	64.2	2 : 1
$\text{Pd}(\text{DECO})_2$, 3	3.4	no conductance
$\text{Pt}(\text{DECO})_2$, 6	64.2	no conductance

2. Crystal structures

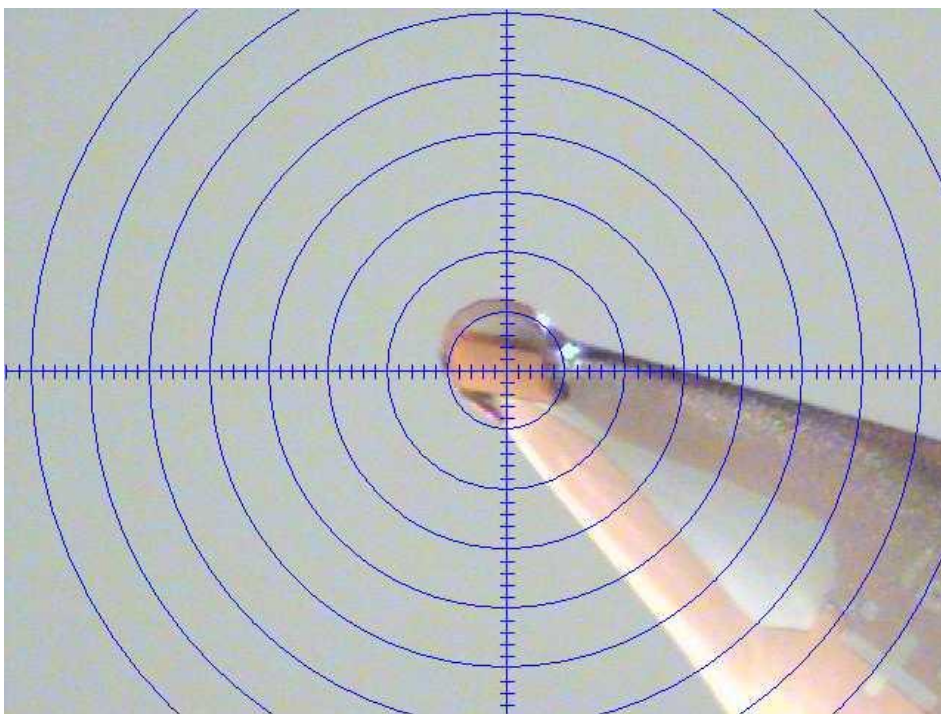
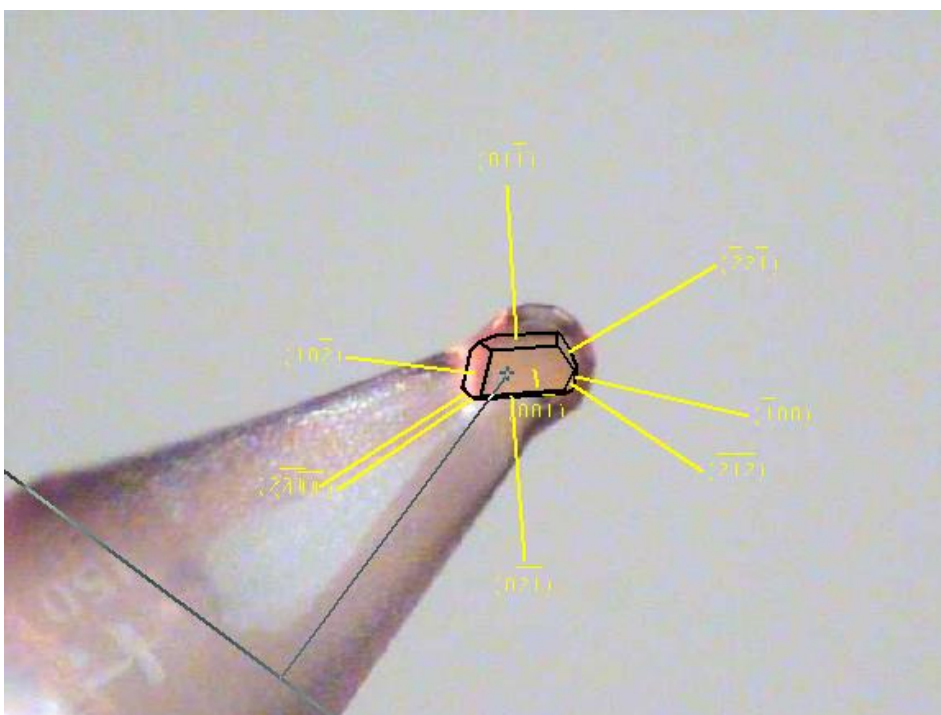
2.1. The cyanoxime HDECO (compound 1)

A - molecular structure and numbering scheme for H(DECO); thermal ellipsoids here and further are drawn at 50% probability. **B** – H-bonded sheet of molecules aligned along *c* direction. **C** – the cyanoxime core showing two planar fragments with the dihedral angle of 53.06° between them; H-atoms are omitted for clarity.



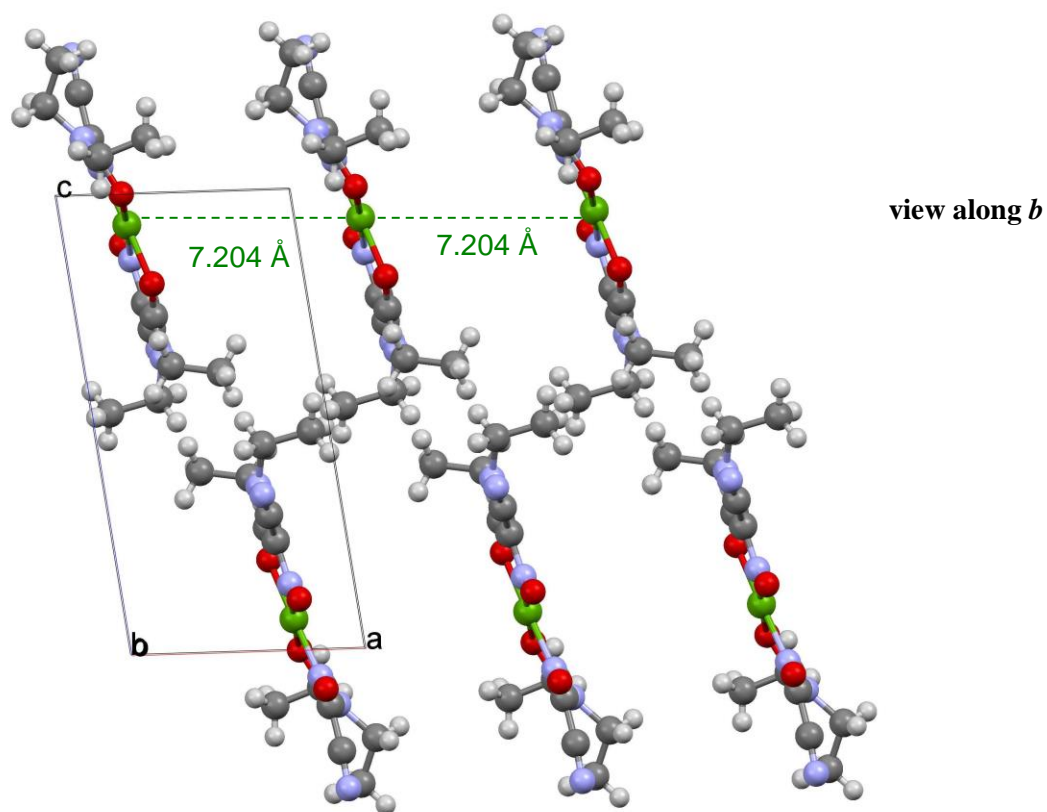
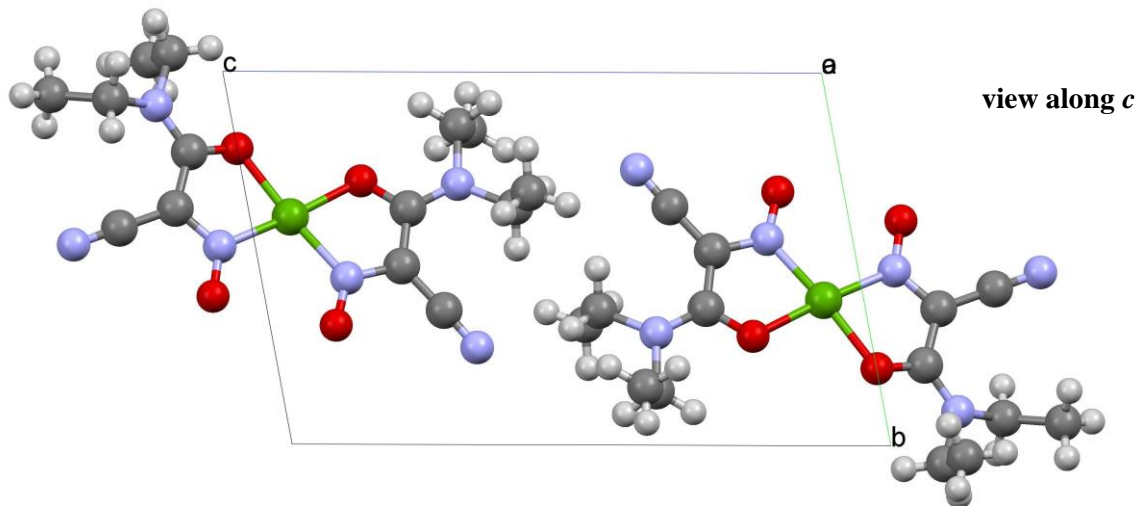
2.2. Crystal data for yellow monomeric $Pt(DECO)_2$ (complex 3).

The videomicroscope photograph of a single crystal of the complex (A), and its face-indexing (B). Crystal of this complex was selected in thick NVH paraton oil and placed into the MiTeGen 150 μm plastic loop for data collection at 120 K.

**A****B**

2.2.1. Crystal packing in the structure of yellow monomeric $Pt(DECO)_2$, (complex 3)

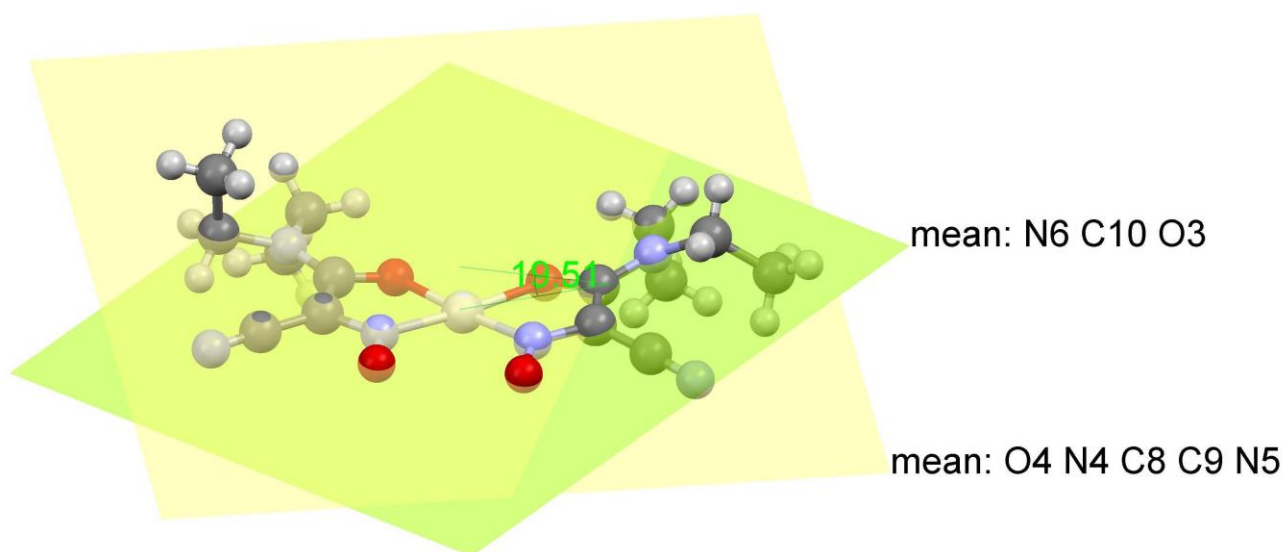
Perspective views of three unit cells along different directions. Units of monomeric $Pt(DECO)_2$ complex form slipped columns along a axis.



Coloring scheme: Pt – green, C – grey, N – blue, O – red, H – white.

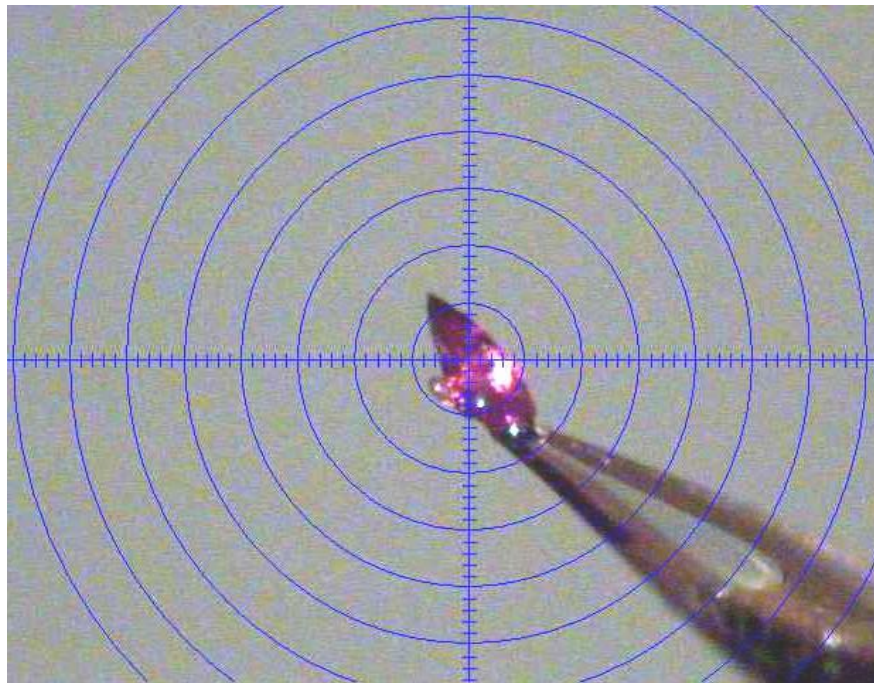
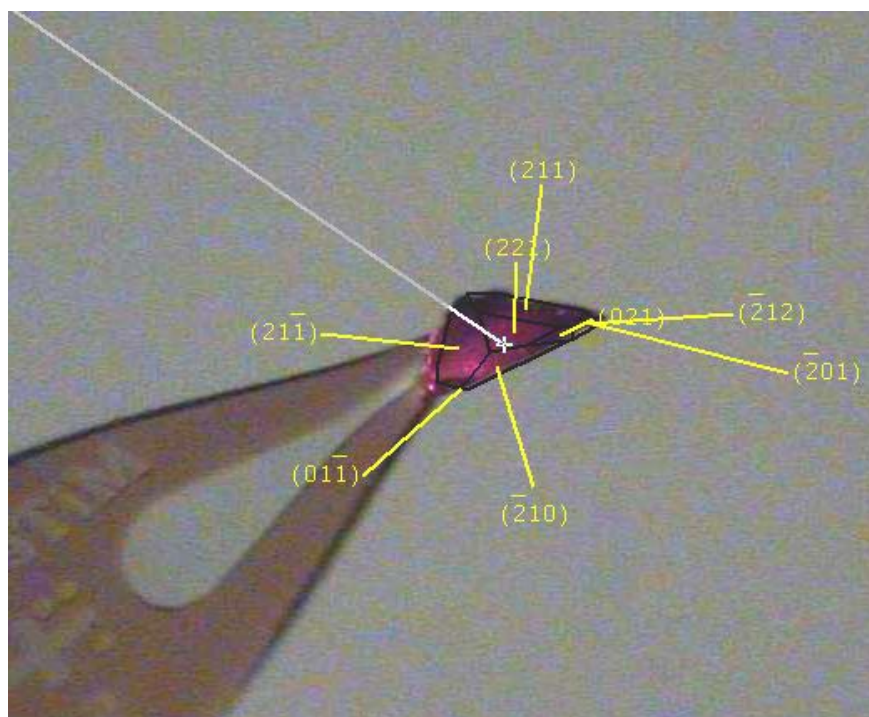
2.2.2. Geometrical features of the cyanoxime anion $DECO^-$ in yellow monomeric $Pt(DECO)_2$ (complex 3).

The dihedral angle between two planes defined in structures of the cyanoxime anion $DECO^-$ (**2**) in yellow monomeric complex **3** is 19.51° .



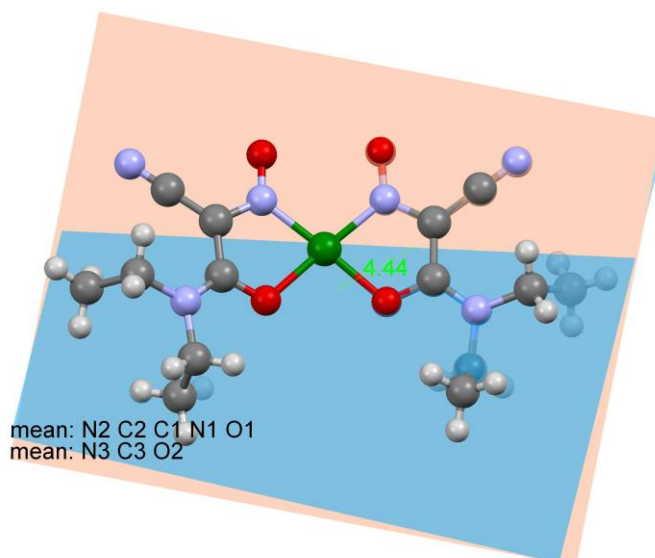
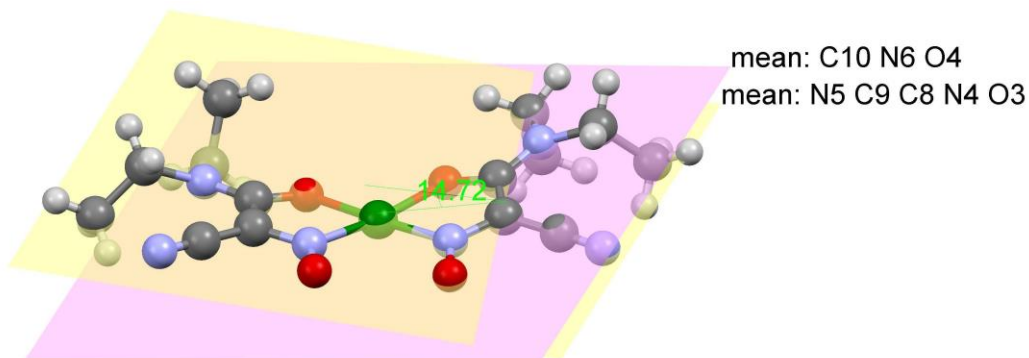
2.3. Crystal data for the red dimer $Pt(DECO)_2$ (complex 4).

The videomicroscope photograph of a single crystal of the complex (**A**), and its face-indexing (**B**). Crystal of this complex was selected in thick NVH paraton oil and placed into the MiTeGen 150 μm plastic loop for data collection at 120 K.

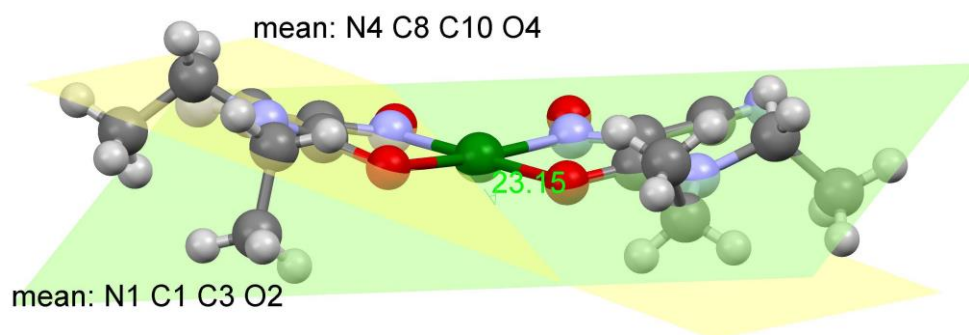
**A****B**

2.3.1. Geometry of cyanoxime anions $DECO^-$ in the structure of red dimeric $Pt(DECO)_2$ (complex 4).

There are two significantly different geometry fragments in the convex-bowl shaped dimer. In both chelate rings the anion **2** is non-planar, but to a different degree: 14.71 and 4.44°.

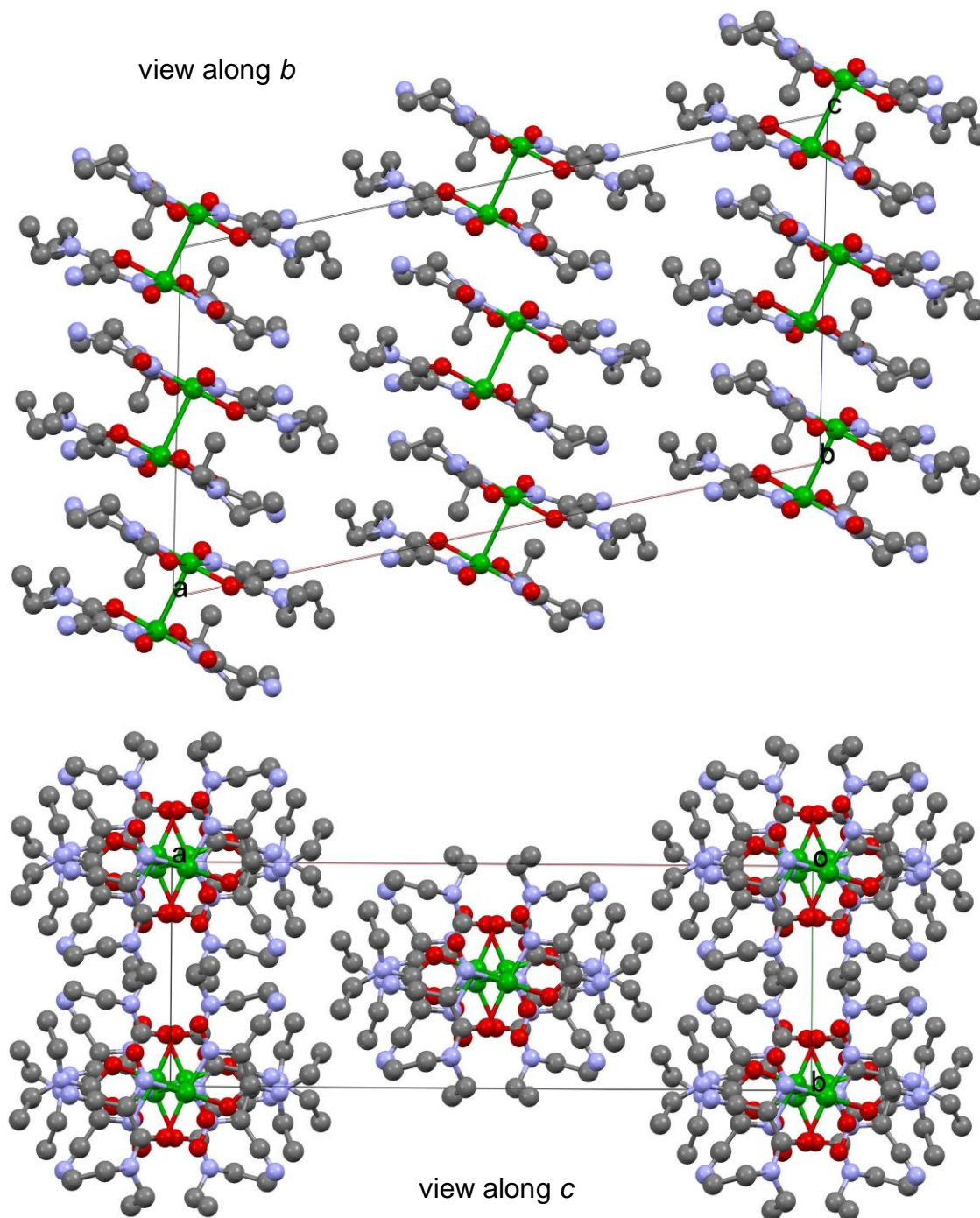


Two chelate rings also form the dihedral angle (23.15°) that defines the bowl-shape of the monomeric unit in the structure of a dimer:



2.3.2. Perspective views of the unit cell content of $Pt(DEC(O)_2)_2$ (4), red dimer

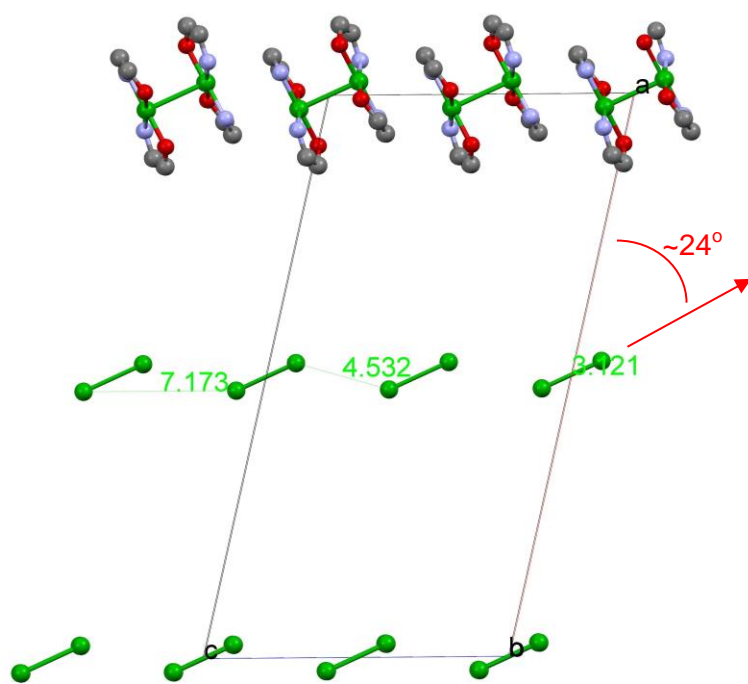
Perspective views of the unit cell content along different directions. H-atoms are omitted for clarity. Units of red $Pt(DEC(O)_2)_2$ polymorph form slipped columns of dimers.



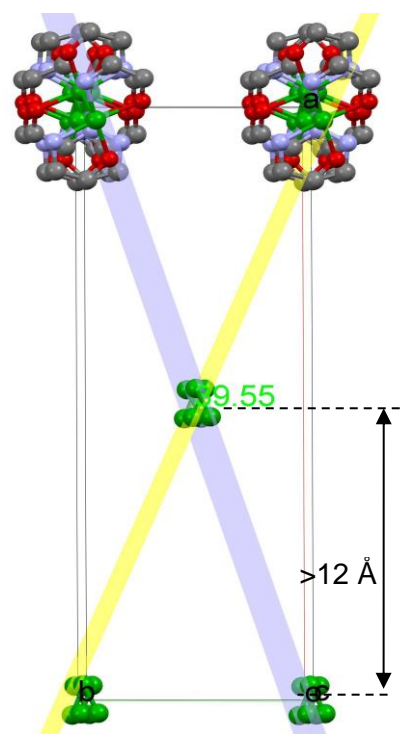
2.3.3. Crystal packing in the structure of red dimeric $Pt(DEC O)_2$ (complex 4) in detail

A – prospective view of 1.5 cells along b -direction showing only one layer of $[PtN_2O_2]$ chelate rings and arrangements of Pt atoms in the structure with interplatinum separations in one slipped column running along b . **B** – same unit cell content view along c showing the tilt angle between two Pt-Pt distances in **4**.

A view along b

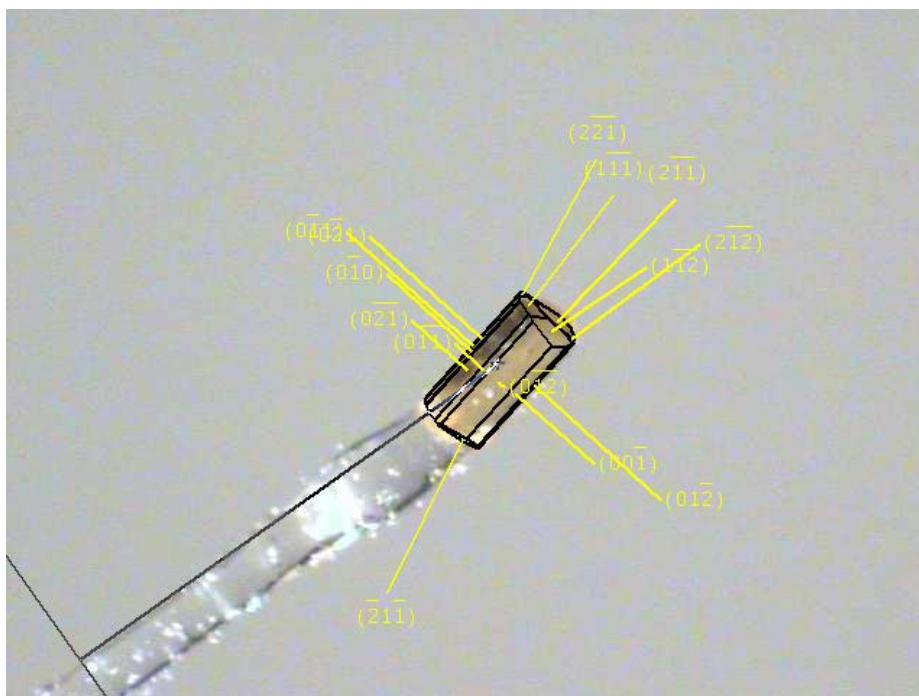
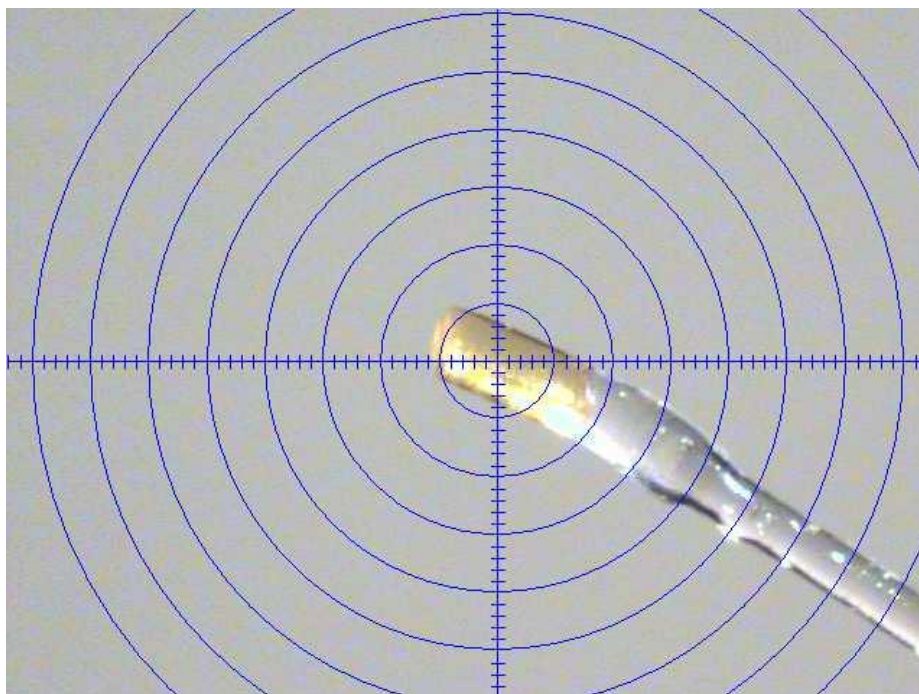


B view along c



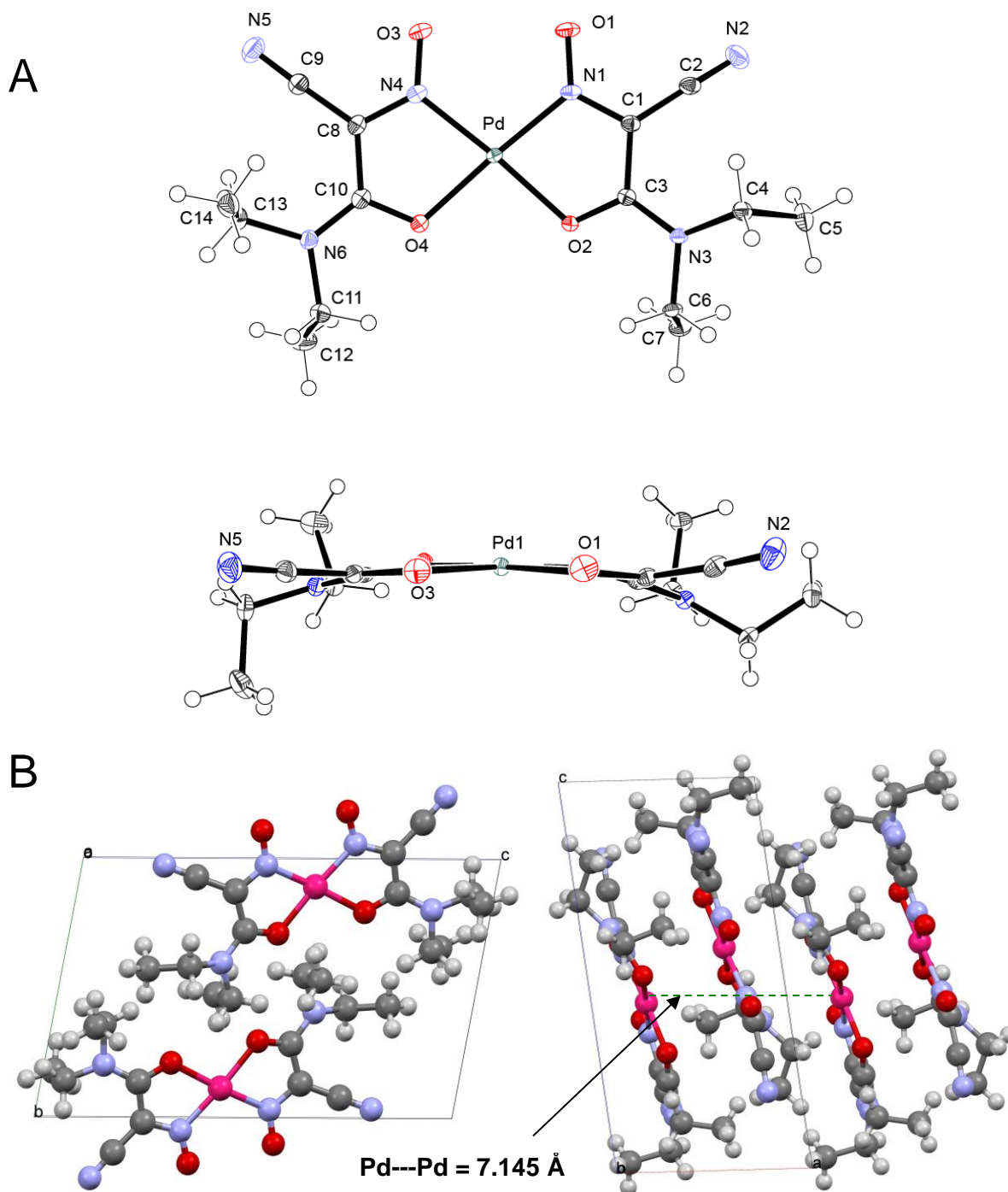
2.4. Crystal data for monomeric yellow $\text{Pd}(\text{DECO})_2$ (complex 6).

Videomicroscope photograph of a single crystal of the complex (A) and its face-indexing (B). Crystal of this complex was selected in thick NVH paraton oil because it was big enough it was mounted on the tip of a thin glass fiber for data collection at 120 K.



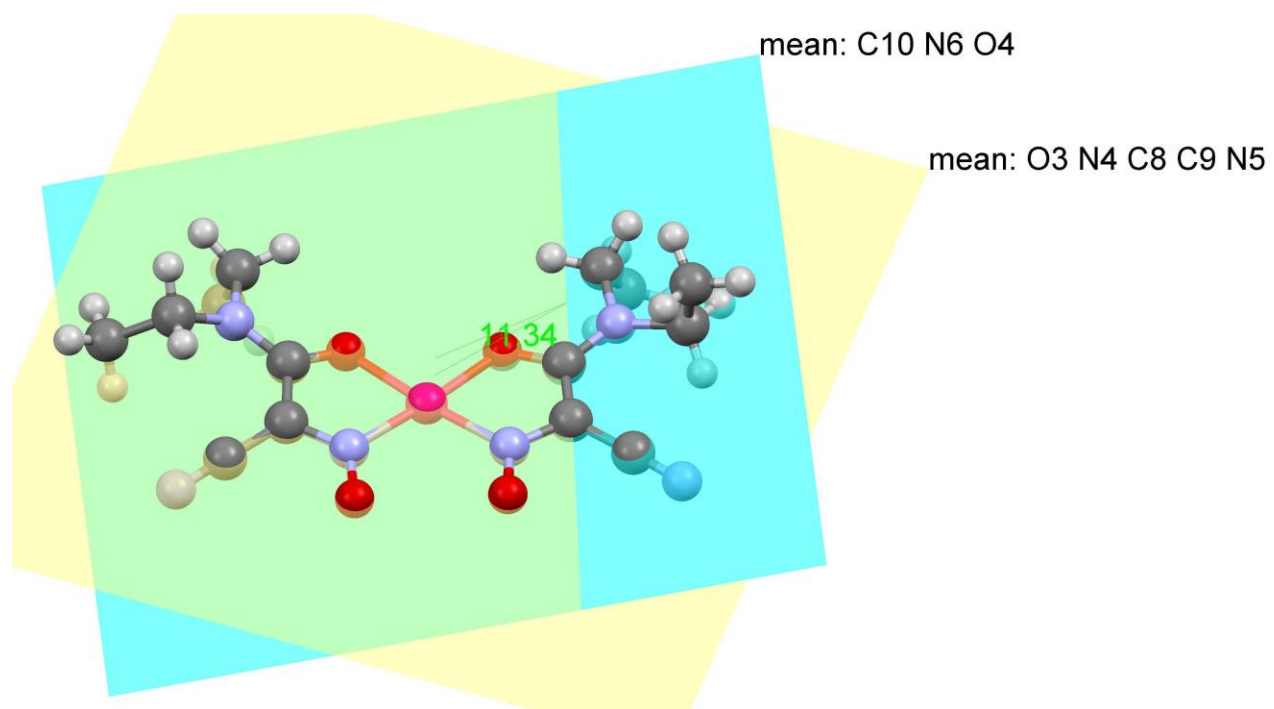
2.4.1 Structure and numbering scheme for Pd(DECO)₂ (complex 6)

A - Molecular structure and numbering scheme for Pd(DECO)₂, **6**, shown in two orthogonal views; **B** - perspective views of two unit cells along different directions.



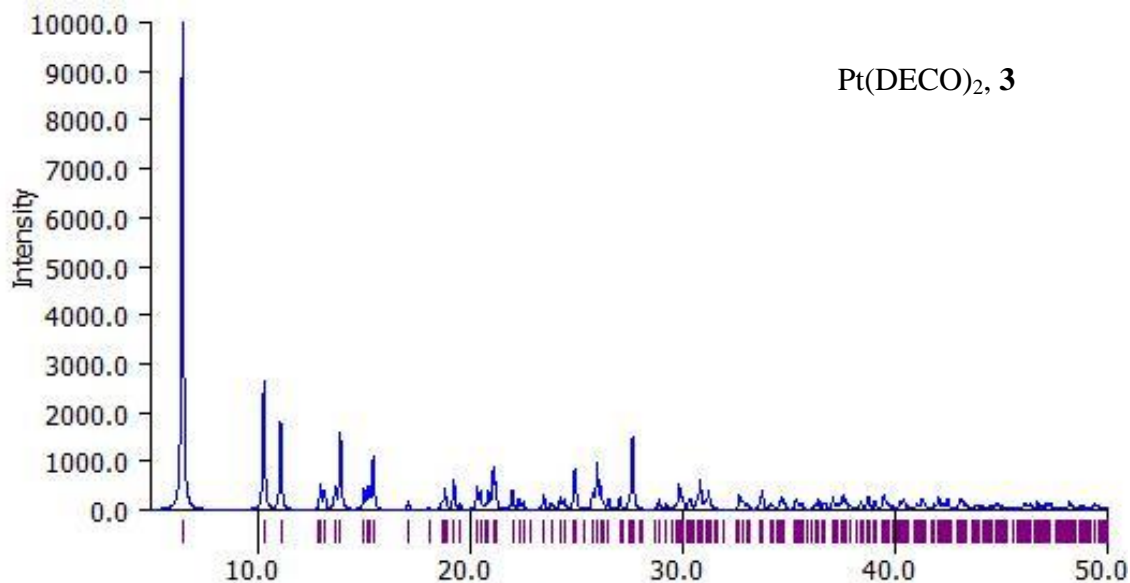
Coloring scheme: Pd – pink, C – grey, N – blue, O – red, H – white.

2.4.2 Geometry of the cyanoxime anion $DECO^-$ in Pd complex 6.

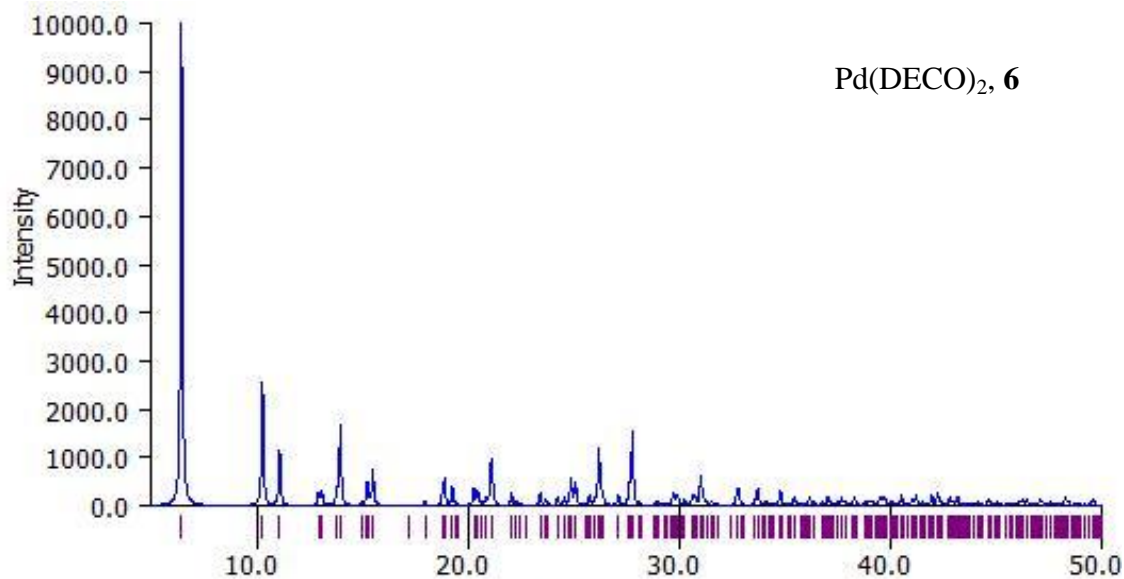


2.4.3 Simulated powder XRD patterns for Pt(DECO)₂, yellow monomer (3), and yellow Pd(DECO)₂ complex (6).

Simulated (based on single-crystal diffraction CIF data) powder XRD patterns for monomeric Pd and Pt-cyanoximates containing DECO anion showing that both complexes are isostructural.



Wavelength: 1.54056



Wavelength: 1.54056

2.5 Crystal data for all studied compounds: H(DECO)(1) and its Pd, Pt complexes 3, 4 and 6.

	HDECO, 1	Pd(DECO) ₂ , 6	Pt(DECO) ₂ , <i>monomer</i> , 3	Pt(DECO) ₂ , <i>dimer</i> , 4
Empirical formula	C ₇ H ₁₁ N ₃ O ₂	C ₁₄ H ₂₀ N ₆ O ₄ Pd	C ₁₄ H ₂₀ N ₆ O ₄ Pt	C ₁₄ H ₂₀ N ₆ O ₄ Pt
Color	colorless	bright yellow	yellow	dark red
Crystal size, mm	0.06 x 0.1 x 0.3	0.29 x 0.17 x 0.09	0.23 x 0.13 x 0.05	0.20 x 0.25 x 0.35
Formula weight	169.19	442.76	531.45	531.45
Temperature, K	120(2)	120(2)	120(2)	120(2)
Crystal system	Monoclinic	Triclinic	Triclinic	Monoclinic
Space group, #	P2(1)/c, 14	P -1, #2	P -1, #2	C2/c, #15
Unit cell, Å, °	a = 8.5424(10) b = 7.9608(10) c = 13.2705(16) α = 90 β = 99.060(2) γ = 90	a = 7.1454(6) b = 9.1247(7) c = 13.9509(11) α = 98.8470(10) β = 94.1610(10) γ = 106.5090(10)	a = 7.2038(4) b = 9.0996(5) c = 13.8997(7) α = 98.9830(10) β = 94.6390(10) γ = 106.3810(10)	a = 27.0687(18) b = 9.1876(6) c = 14.3089(10) α = 90 β = 102.9600(10) γ = 90
Unit cell volume, Å ³	891.19(19)	855.21(12)	855.91(8)	3467.9(4)
Z	4	2	2	8
Density (calc.) Mg/m ³	1.261	1.719	2.062	2.036
Absorp. coeff., mm ⁻¹	0.095	1.118	8.230	8.125
F(000)	360	448	512	2048
Θ range, °	2.41 to 27.86	1.49 to 26.73	1.50 to 28.28	1.54 to 30.99
Index ranges	-11 ≤ h ≤ 11 -10 ≤ k ≤ 10 -17 ≤ l ≤ 17	-9 ≤ h ≤ 9 -11 ≤ k ≤ 11 -17 ≤ l ≤ 17	-9 ≤ h ≤ 9 -12 ≤ k ≤ 12 -18 ≤ l ≤ 18	-39 ≤ h ≤ 38 -13 ≤ k ≤ 13 -20 ≤ l ≤ 20
Structures solution			<i>Direct</i>	
Reflections collected	9987	10130	11281	26242
Independent reflections	2123 [R(int)=0.0470]	3599 [R(int)=0.0183]	4234 [R(int)=0.0228]	5510 [R(int)=0.0364]
Completeness to Θ, (%)	27.86° (99.6)	26.73° (98.9)	28.28° (99.4)	30.99 (99.6)
Absorption correction	None	Numerical	Numerical	Numerical

T_{\max} and T_{\min}	n/a	1.000 and 0.9176	0.6843 and 0.3036	0.2930 and 0.1630
<i>Refinement method</i>		<i>Full-matrix least-squares on F^2</i>		
Data/restraints/parameters	2123 / 0 / 112	3599 / 0 / 230	4234 / 0 / 306	5510 / 0 / 230
Goodness-of-fit on F^2	1.030	1.109	1.114	1.115
Final R indices [$I > 2\sigma(I)$]	R1 = 0.0404, wR2 = 0.0904	R1 = 0.0185 wR2 = 0.0405	R1 = 0.0195 wR2 = 0.0366	R1 = 0.0258 wR2 = 0.046
R indices (all data)	R1 = 0.0622, wR2 = 0.1011	R1 = 0.0198 wR2 = 0.0412	R1 = 0.0225 wR2 = 0.0374	R1 = 0.0375 wR2 = 0.0496
Largest peak/ hole, e. \AA^{-3}	0.241 / -0.230	0.412 / -0.610	0.987 / -1.582	1.599 / -1.088
Structures volume, \AA^3 (%):	547.3 (61.4)	560.8 (65.6)	557.8 (65.2)	2256.7 (65.1)

2.6 Selected values of bond lengths and valence angles

Selected values of bond lengths and valence angles in the crystal structures of a new cyanoxime and its Pd,Pt-complexes. Numbering schemes can be found in Figure 2 and **S6, 14**.

Compound	Bond length, Å		Valence angle, °	
HDECO (1)	C(1)-N(1)	1.2844(17)	N(1)-C(1)-C(2)	122.72(12)
	N(1)-O(1)	1.3719(14)	N(1)-C(1)-C(3)	120.24(12)
	C(1)-C(2)	1.4453(19)	C(2)-C(1)-C(3)	116.37(11)
	C(1)-C(3)	1.5031(18)	N(2)-C(2)-C(1)	179.28(16)
	C(2)-N(2)	1.1449(18)	O(2)-C(3)-N(3)	124.71(12)
	C(3)-O(2)	1.2407(15)	O(2)-C(3)-C(1)	115.34(12)
	C(3)-N(3)	1.3269(17)	C(1)-N(1)-O(1)	111.53(11)
	C(4)-N(3)	1.4726(17)	C(3)-N(3)-C(4)	124.91(11)
	C(6)-N(3)	1.4743(17)	C(3)-N(3)-C(6)	118.29(11)
Yellow Pt(DECO)₂ monomer, (3)	Organic ligand:			
	C(1)-N(1)	1.359(4)	N(1)-C(1)-C(2)	117.4(3)
	C(8)-N(4)	1.352(4)	N(4)-C(8)-C(9)	118.8(2)
	N(1)-O(1)	1.249(3)	N(1)-C(1)-C(3)	113.7(2)
	N(4)-O(4)	1.249(3)	N(4)-C(8)-C(10)	114.5(2)
	C(1)-C(2)	1.426(4)	C(2)-C(1)-C(3)	128.8(3)
	C(8)-C(9)	1.416(4)	C(9)-C(8)-C(10)	126.2(3)
	C(1)-C(3)	1.463(4)	N(2)-C(2)-C(1)	177.6(3)
	C(8)-C(10)	1.455(4)	N(5)-C(9)-C(8)	176.3(3)
	C(2)-N(2)	1.150(4)	O(2)-C(3)-N(3)	118.9(3)
	C(9)-N(5)	1.147(4)	O(3)-C(10)-N(6)	119.6(2)
	C(3)-O(2)	1.283(3)	O(2)-C(3)-C(1)	115.9(3)
	C(10)-O(3)	1.280(3)	O(3)-C(10)-C(8)	116.4(2)
	C(3)-N(3)	1.321(4)	O(1)-N(1)-C(1)	119.9(2)
	C(10)-N(6)	1.325(3)	O(4)-N(4)-C(8)	120.4(2)
	Metal center:			
	N(1)-Pt(1)	1.961(2)	N(1)-Pt(1)-N(4)	102.81(10)
N(4)-Pt(1)	1.969(2)	N(1)-Pt(1)-O(2)	80.54(9)	
O(2)-Pt(1)	2.0233(19)	N(4)-Pt(1)-O(2)	176.14(8)	
O(3)-Pt(1)	2.0321(18)	N(1)-Pt(1)-O(3)	175.22(9)	
		N(4)-Pt(1)-O(3)	81.05(9)	
		O(2)-Pt(1)-O(3)	95.51(7)	

Table S20 (continued) Selected values of bond lengths and valence angles in the crystal structures of a new cyanoxime and its Pd, Pt-complexes.

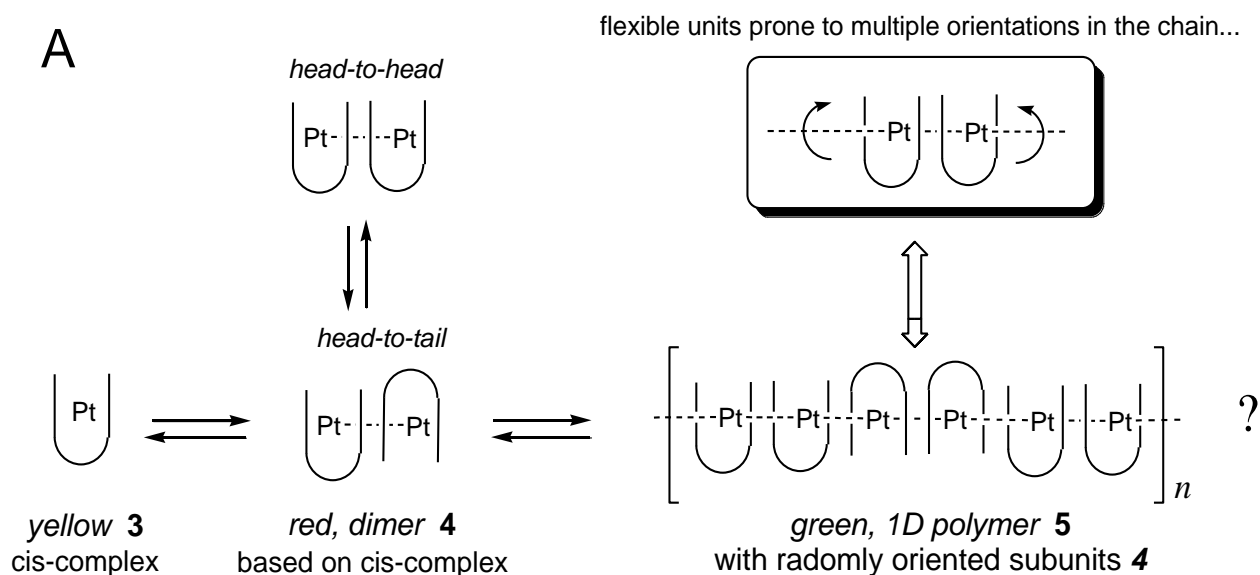
Compound	Bond length, Å		Valence angle, °	
	Organic ligand:			
Red Pt(DECO)₂ Dimer (4)	C(1)-N(1)	1.357(4)	N(1)-C(1)-C(2)	117.6(3)
	C(8)-N(4)	1.354(4)	N(4)-C(8)-C(9)	117.6(3)
	N(1)-O(1)	1.239(3)	N(1)-C(1)-C(3)	114.8(3)
	N(4)-O(4)	1.240(3)	N(4)-C(8)-C(10)	113.9(3)
	C(1)-C(2)	1.423(5)	C(2)-C(1)-C(3)	127.6(3)
	C(8)-C(9)	1.428(4)	C(9)-C(8)-C(10)	128.2(3)
	C(1)-C(3)	1.451(5)	N(2)-C(2)-C(1)	179.4(5)
	C(8)-C(10)	1.457(5)	N(5)-C(9)-C(8)	178.0(4)
	C(2)-N(2)	1.144(5)	O(2)-C(3)-N(3)	119.0(3)
	C(9)-N(5)	1.144(4)	O(4)-C(10)-N(6)	118.4(3)
	C(3)-O(2)	1.284(4)	O(2)-C(3)-C(1)	116.1(3)
	C(10)-O(3)	1.290(4)	O(4)-C(10)-C(8)	116.4(3)
	C(3)-N(3)	1.322(4)	O(1)-N(1)-C(1)	120.4(3)
	C(10)-N(6)	1.322(4)	O(3)-N(4)-C(8)	120.4(3)
	Metal center:			
	N(1)-Pt(1)	1.969(3)	N(1)-Pt(1)-N(4)	102.26(11)
	N(4)-Pt(1)	1.969(3)	N(1)-Pt(1)-O(2)	80.60(10)
	O(2)-Pt(1)	2.029(2)	N(4)-Pt(1)-O(2)	177.04(10)
	O(4)-Pt(1)	2.036(2)	N(1)-Pt(1)-O(4)	172.71(10)
			N(4)-Pt(1)-O(3)	80.60(10)
			O(2)-Pt(1)-O(4)	96.48(9)
	Organic ligand:			
Yellow, monomer Pd(DECO)₂ (6)	C(1)-N(1)	1.345(2)	N(1)-C(1)-C(2)	118.73(15)
	C(8)-N(4)	1.350(2)	N(4)-C(8)-C(9)	117.26(15)
	N(1)-O(1)	1.2464(18)	N(1)-C(1)-C(3)	114.93(15)
	N(4)-O(3)	1.2479(18)	N(4)-C(8)-C(10)	114.25(15)
	C(1)-C(2)	1.427(2)	C(2)-C(1)-C(3)	125.74(15)
	C(8)-C(9)	1.432(2)	C(9)-C(8)-C(10)	128.38(16)
	C(1)-C(3)	1.464(2)	N(2)-C(2)-C(1)	176.3(2)
	C(8)-C(10)	1.469(2)	N(5)-C(9)-C(8)	177.5(2)
	C(2)-N(2)	1.149(2)	O(2)-C(3)-N(3)	119.91(15)
	C(9)-N(5)	1.150(2)	O(4)-C(10)-N(6)	119.00(15)
	C(3)-O(2)	1.280(2)	O(2)-C(3)-C(1)	116.62(15)
	C(10)-O(4)	1.278(2)	O(4)-C(10)-C(8)	116.22(15)
	C(3)-N(3)	1.323(2)	O(1)-N(1)-C(1)	121.15(15)
	C(10)-N(6)	1.326(2)	O(3)-N(4)-C(8)	120.90(14)

Table S20 (continued). Selected values of bond lengths and valence angles in the crystal structures of a new cyanoxime and its Pd,Pt-complexes

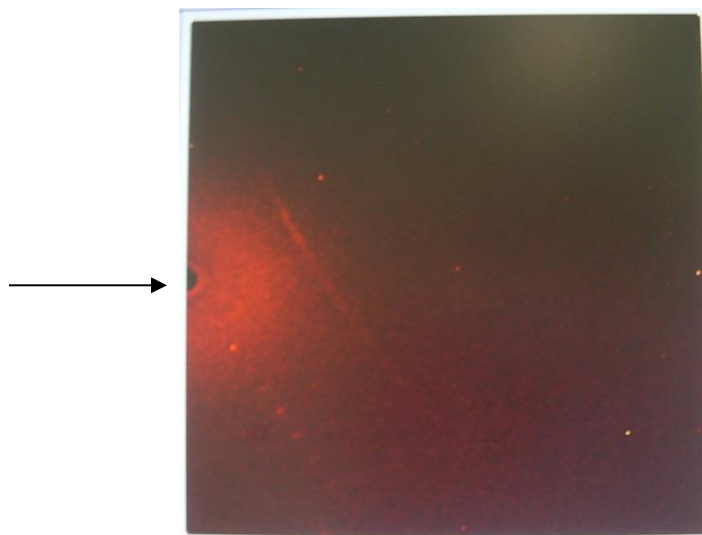
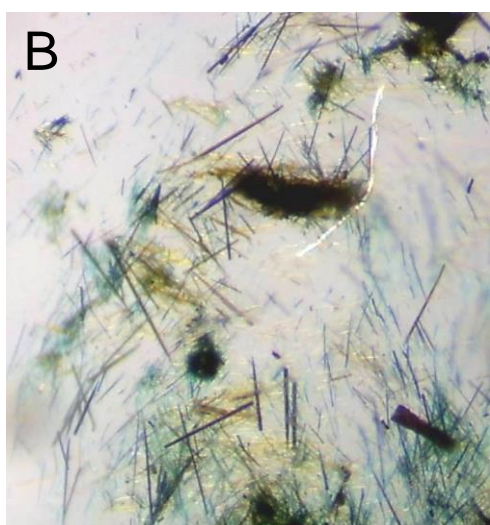
Compound	Bond length, Å		Valence angle, °	
	Metal center:			
	N(1)-Pd(1)	1.9846(15)	N(4)-Pd(1)-N(1)	102.11(6)
	N(4)-Pd(1)	1.9798(14)	N(4)-Pd(1)-O(4)	80.67(5)
	O(2)-Pd(1)	2.0358(12)	N(1)-Pd(1)-O(4)	176.52(5)
	O(4)-Pd(1)	2.0300(12)	N(4)-Pd(1)-O(2)	175.55(5)
			N(1)-Pd(1)-O(2)	81.46(5)
			O(4)-Pd(1)-O(2)	95.67(5)

2.7 Building blocks rotational flexibility around metallophilic Pt---Pt vector poses problem during crystal growth.

Tentative plausible explanation of difficulties encountered during attempts of crystal growth of 1D polymeric Pt-cyanoximates: flexibility of mutual orientation of dimeric weakly bound $[\text{PtL}_2]_2$ units **4** (believed to be the building blocks – monomer of the polymer) complicates formation of a repetitive pattern necessary for the formation of 3D-ordered structure (**A**). Lack of the latter gives no diffraction pattern (**B**) with occasional random spots not suitable even unit cell determination. Submitted for the synchrotron studies at APS (Berkeley, CA) thin needles did not produce suitable data set either.



Dark green dichroic needles of **5** that and actual picture of a random frame from the diffractometer:

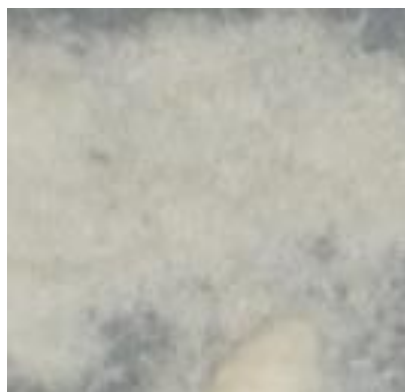


3 Microscopy images of crystals of studied complexes

3.4 Samples of known and established 1D coordination Pt-polymers

Actual microscopic photographs (at 40x) of “control” samples of known and established 1D coordination polymers: **A** – $\text{K}_2[\text{Pt}(\text{CN})_4]$, KCP, **B** – $\text{K}_2[\text{Pt}(\text{CN})_4] \cdot 0.3 \text{ Br} \cdot \text{H}_2\text{O}$, POCP, **C** – Magnus’ Green Salt, MGS, $[\text{Pt}(\text{NH}_3)_4][\text{PtCl}_4]$.

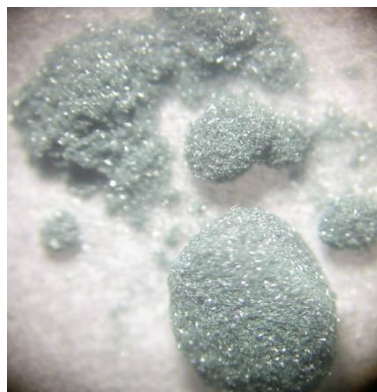
The POCP sample represents mixed valence Pt(II)/Pt(IV) complex that exhibits metallic conductivity, while KCP and MGS are very poor electric conductors at the very bottom range for semiconductors. No reasonably strong communications between Pt-centers in the latter compounds exists.

A

off-white crystals lustrous

B

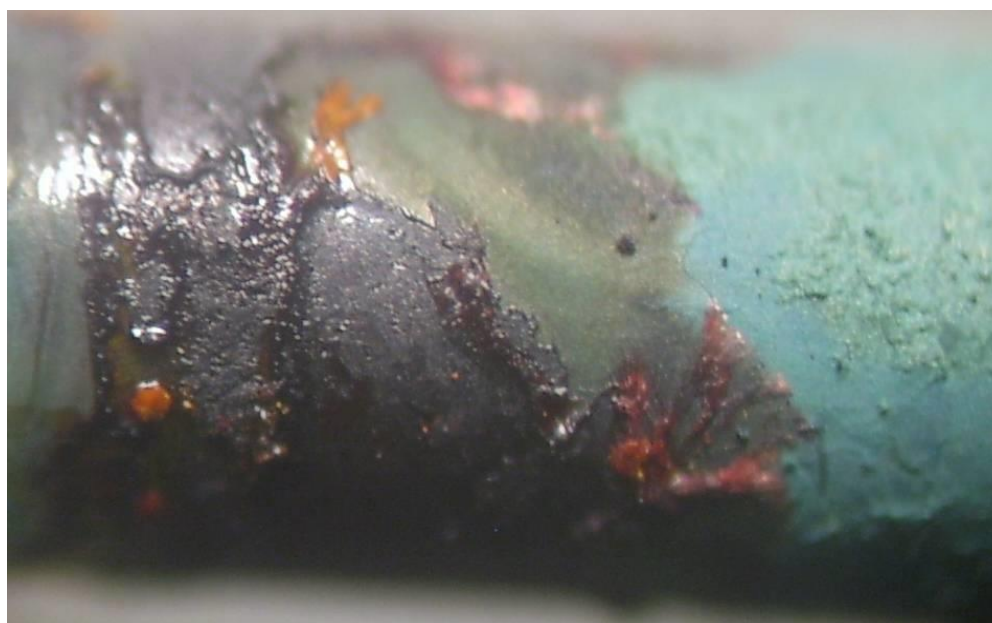
copper-like shiny needles

C

green crystals

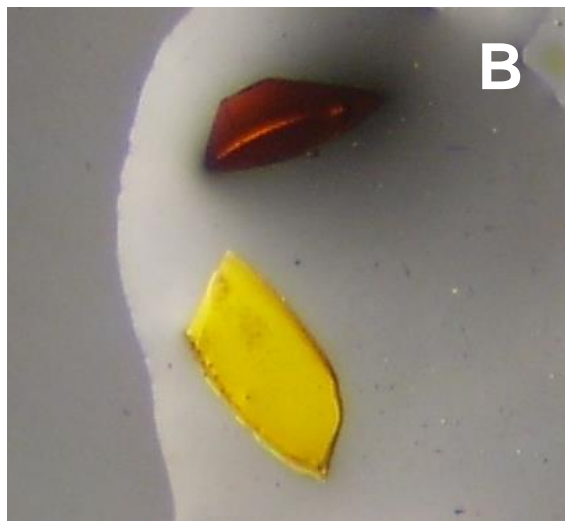
3.5 *Optical microscopy images of crystals in Pt - DECO system.*

Actual photographs of a fragment of glassware with dried solution from the Pt-DECO system at 40x magnification. Clearly seen three differently colored species: yellow – monomeric complex **3**, structure of which has been determined, red – dimeric complex **4**, and green – presumably 1D polymeric complex **5**, structure of which has not been determined yet. It is believed that this has similar to Magnus Green Salt like columnar structure.



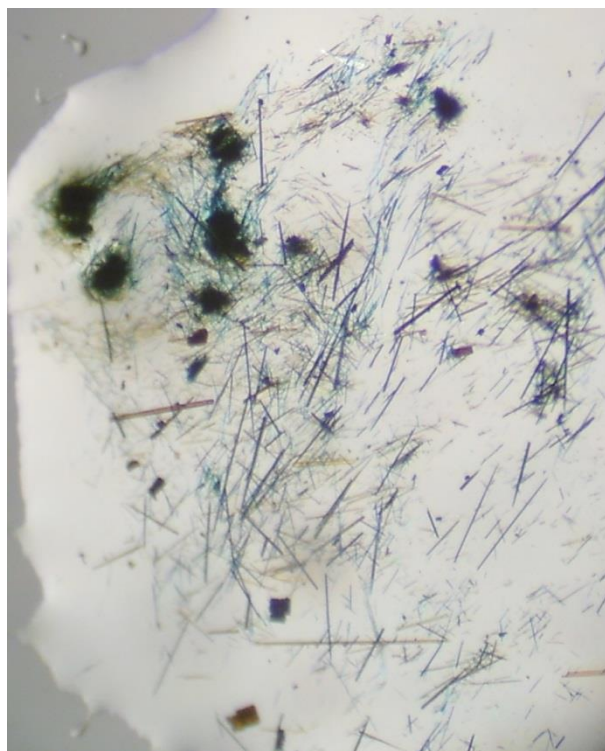
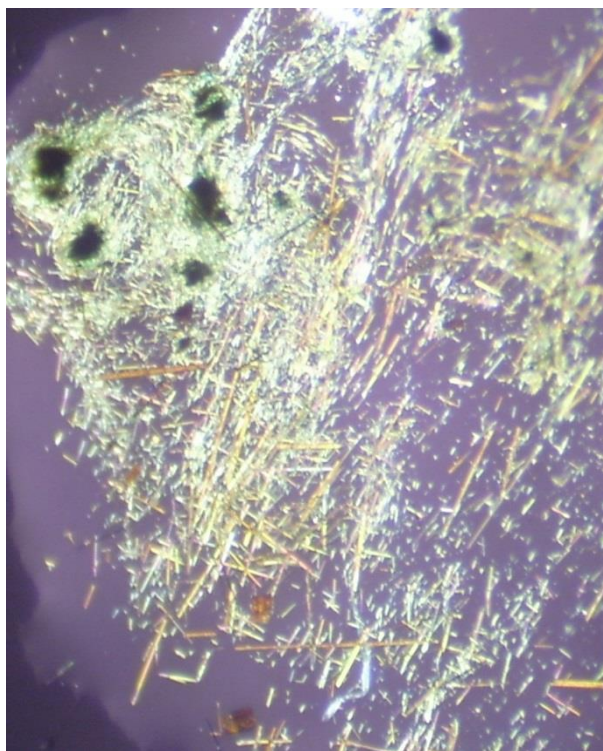
3.6 Optical microscope images of all three polymorphs of $Pt(DECO)_2$

A – yellow monomer **3** and green 1D polymer **5** (as needle habitus crystals on a paper filter), **B** – yellow monomer **3** and red dimer **4**, **C** – all three polymorphs together. Both **B** and **C** pictures are taken in the immersion NVH oil.



3.7 Optical microscope images of polymeric $\text{Pt}(\text{DECO})_2$

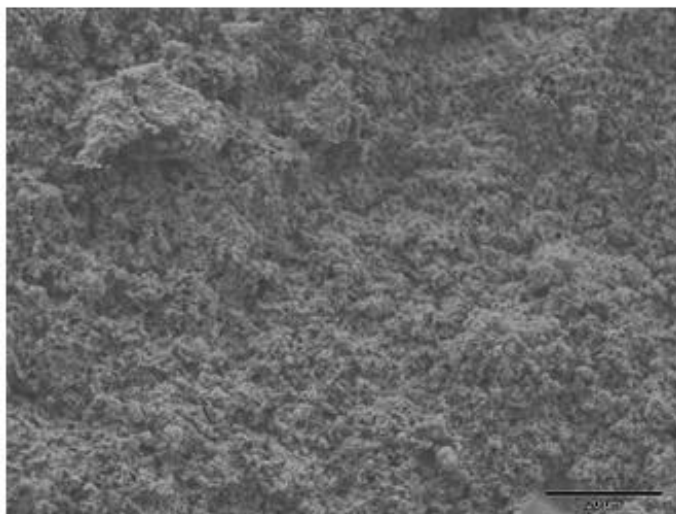
Microscope photographs of polymeric $[\text{Pt}(\text{DECO})_2]_n$ (**5**) at 40x magnification showing pronounced dichroism of the coordination polymer consistent with its 1D structure. Sample is in the immersion oil: **A** – dark-green color in reflected light, and **B** – yellow-brown in passing light.

A**B**

3.8 Scanning Electron Microscopy images of 1D polymer

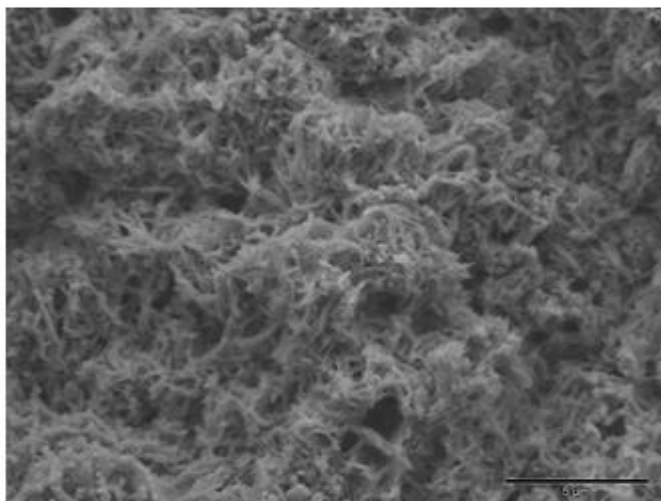
Representative SEM images of the dark-green 1D polymeric complex $[\text{Pt}(\text{DECO})_2]_n$ (**5**) at different magnifications. Shown homogeneous fibrous texture of the complex at $5\ \mu\text{m}$ resolution; no inclusions or solid phases of foreign impurities can be seen from this and four other randomly selected for viewing areas.

Area One



20 μm

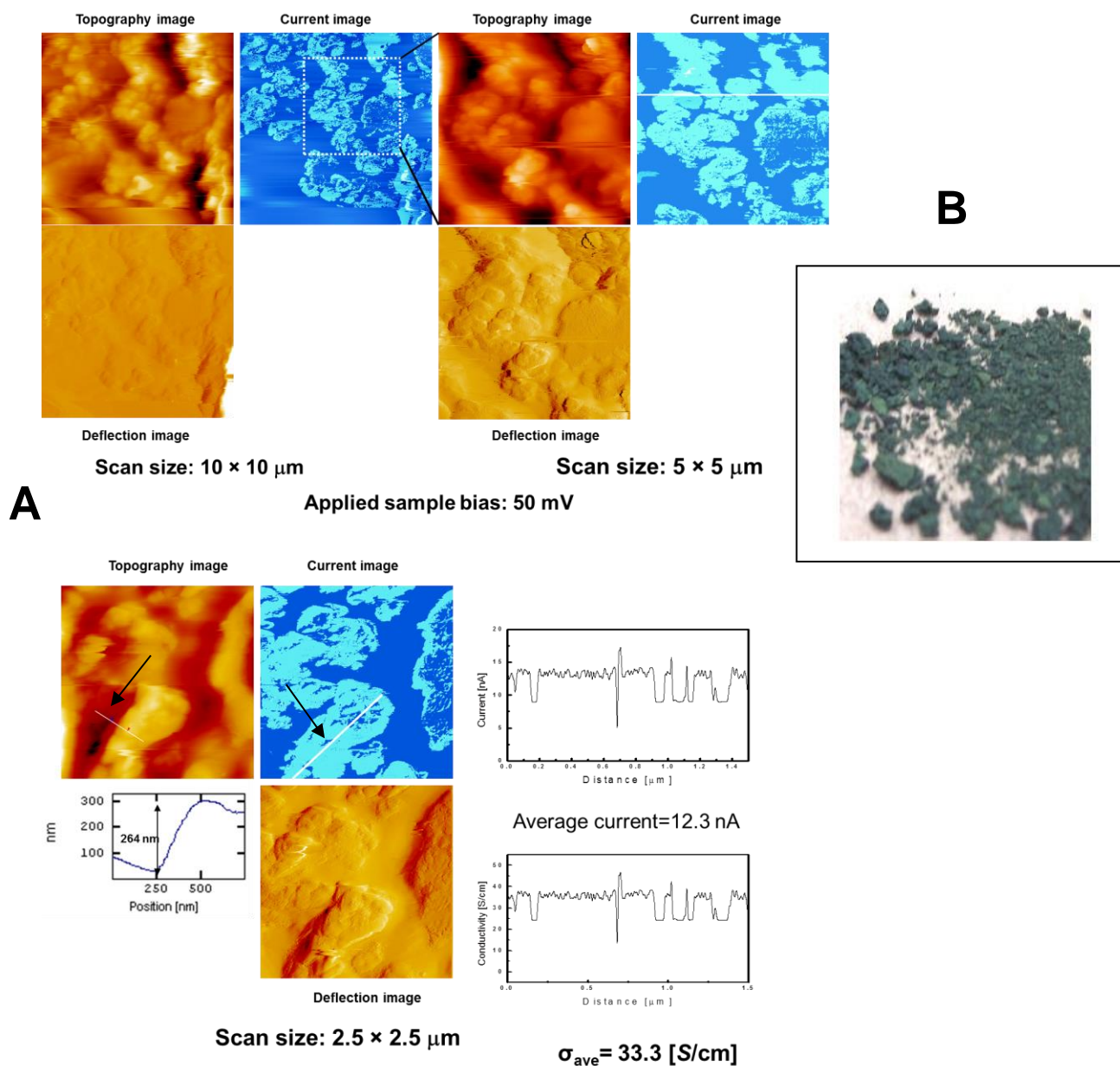
Area One



5 μm

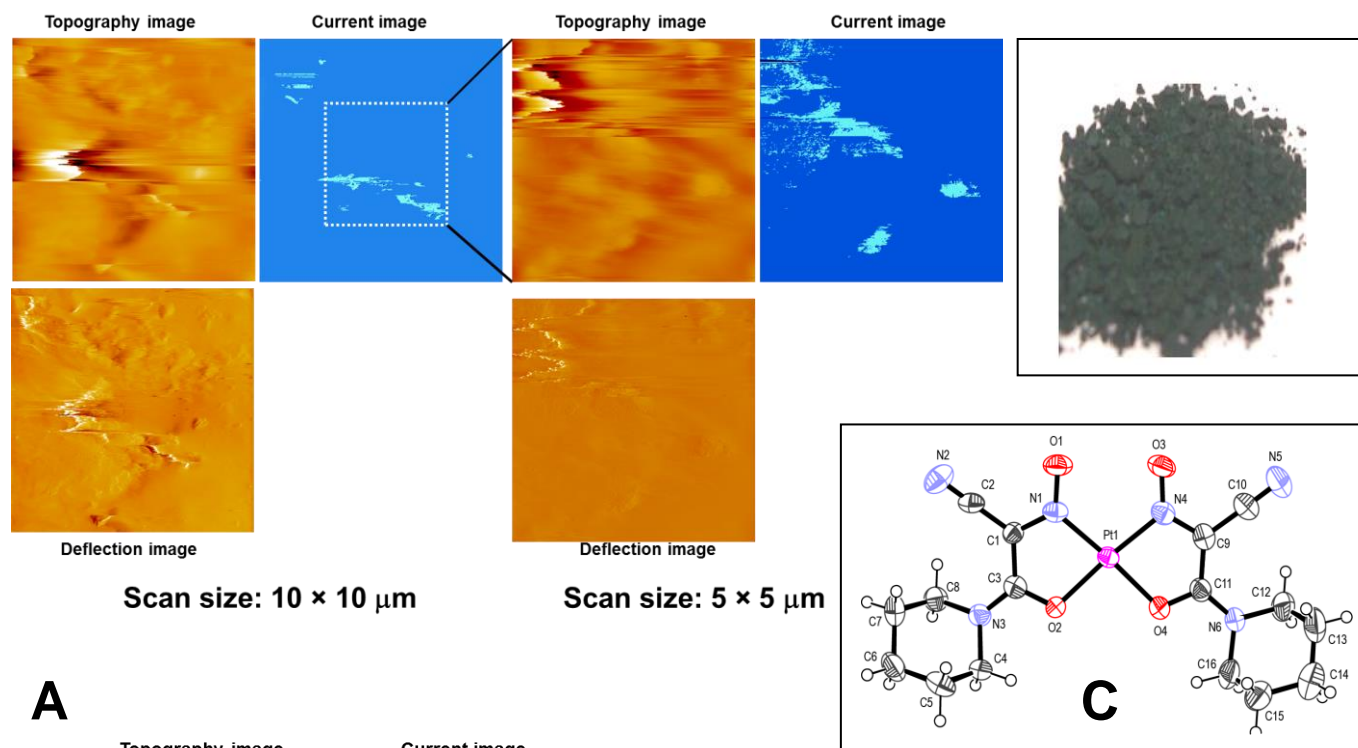
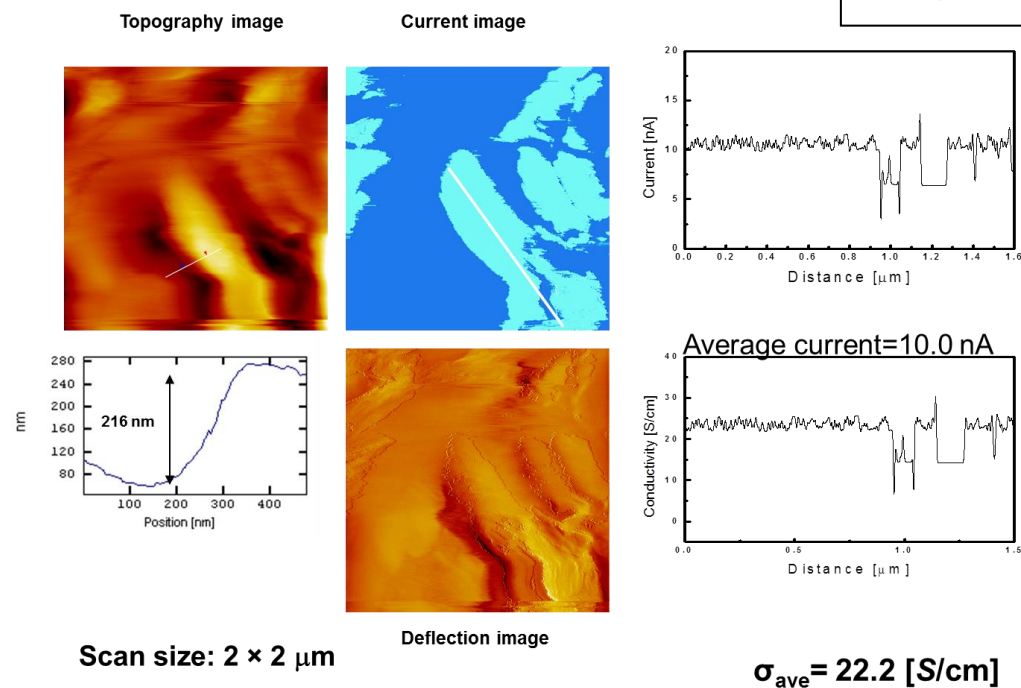
3.9 Scanning Electron Microscopy images and solid state electrical conductivity of analogous Pt-cyanoximates.

A – data for a dark-green polymeric $[\text{Pt}(\text{MCO})_2]_n$ complex at different scan sizes showing details of its electrical conductivity measurements; **B** – actual optical microscope photograph of the compound at 40x magnification;



White lines indicate places of the Ir-tip dragging through the surface of the complex.

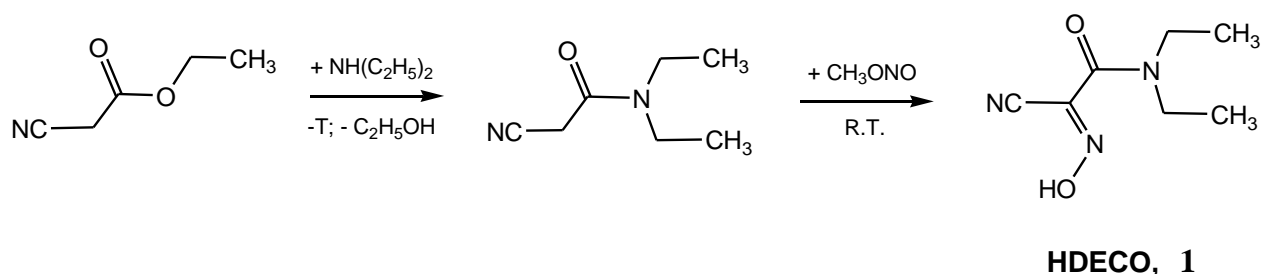
A – data for a dark-green polymeric $[\text{Pt}(\text{PiPCO})_2]_n$ complex at different scan sizes showing details of its electrical conductivity measurements; **B** – actual optical microscope photograph of the compound at 40x magnification; **C** - crystal structure of the yellow monomeric $\text{Pt}(\text{PiPCO})_2$ complex [was reported in *Inorganica Chimica Acta* 385 (2012) 1–20].

B**A**

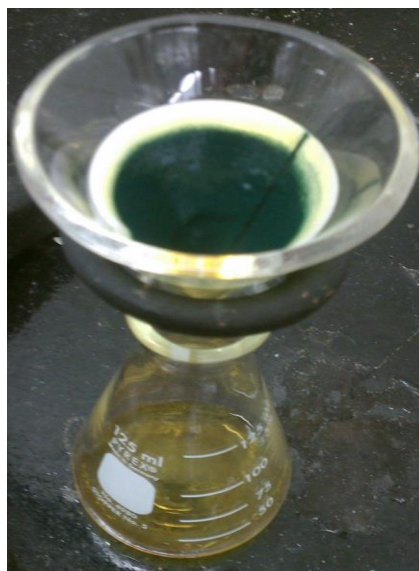
4 Synthesis (additional information)

4.4 HDECO (compound 1)

The cyanoxime ligand – 2-oximino-2-cyano-N,N'-diethylacetamide (**1**, HDECO) – was obtained in high yield according to known procedures from the respective diethylamide as shown in Scheme below. The pure compound represents clear, ice-looking crystals soluble in most organic solvents except hydrocarbons.

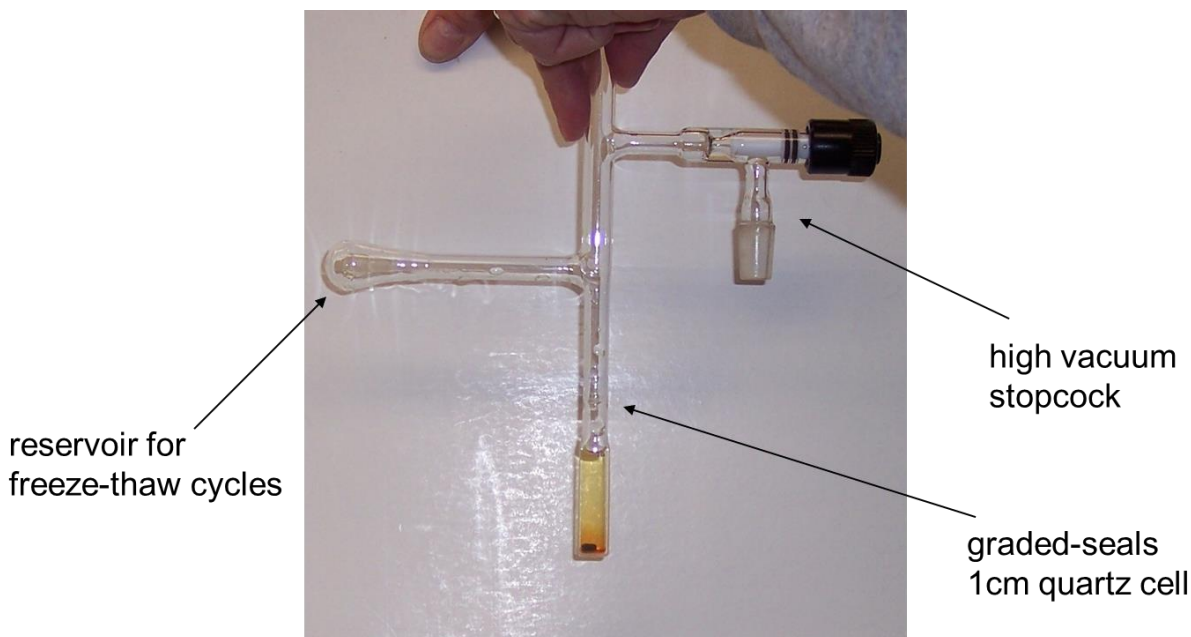


Actual photographs of some of the compounds made. **A** - flask with crystallized pure cyanoxime H(DECO), **1**, used for the NMR spectroscopic studies and synthesis of complexes; **B** – filtering of pure, 1D-polymeric [Pt(DECO)₂]_n complex **5**, that appeared to be a very fine green powder; **C** – yellow microcrystalline powder of Pd(DECO)₂ complex **6**, which was obtained as non-aggregating compound for control purposes.

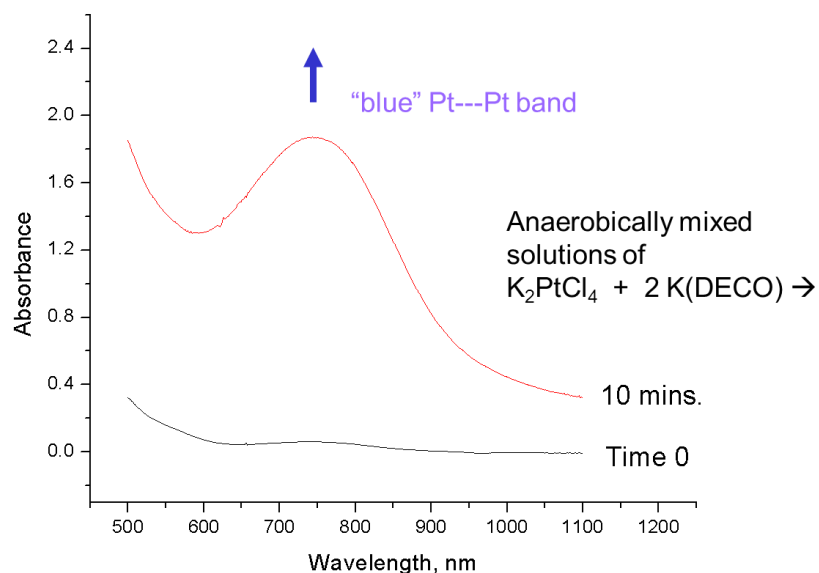
A**B****C**

4.5 Synthesis of $[Pt(DECO)_2]_n$ (5) under air-free conditions.

Anaerobic preparation of $[Pt(DECO)_2]_n$ using custom made 1 cm quartz cuvette. Here all ingredients prior to mixing can be independently dissolved (in water in this case) and via freeze/thaw cycles deaerated. The cuvette is filled with argon at room temperature and components – red solution of $K_2[PtCl_4]$ and yellow solution of $K(DECO)$ – were mixed together by tilting the cuvette. A miniature stirbar at the bottom of cuvette allows thorough mixing during the reaction.

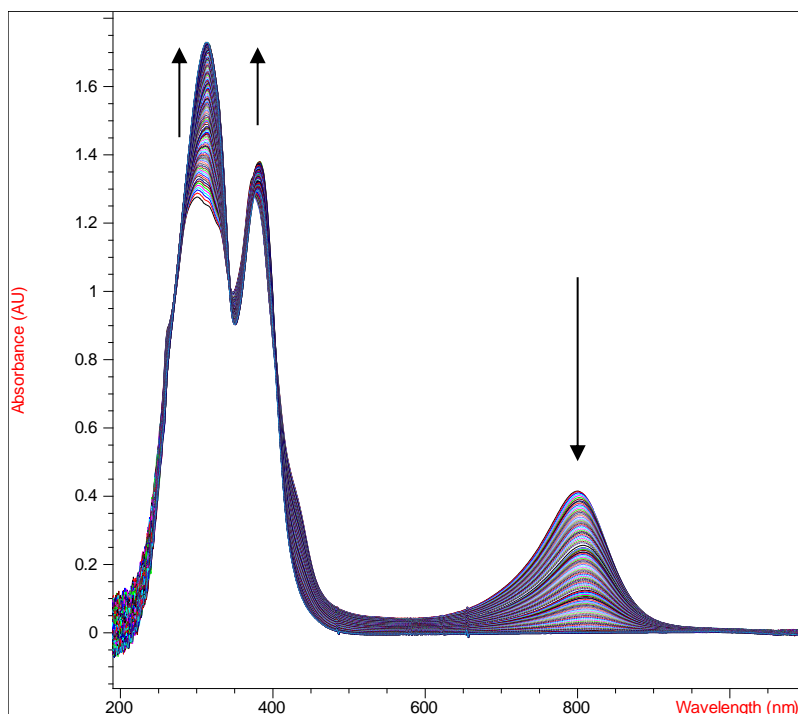
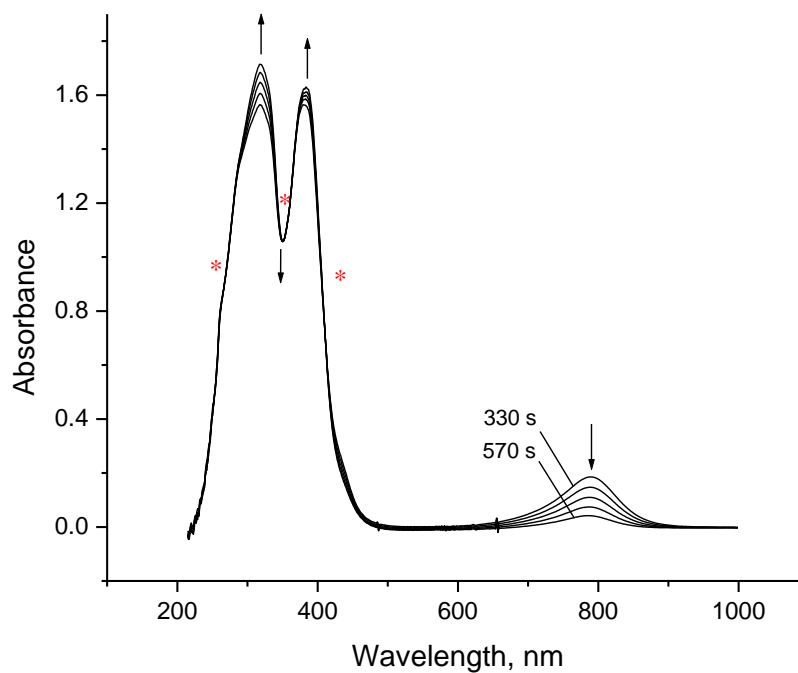


Within ~10 min appearance of the green color was clearly detected visually and spectrophotometrically.



4.6 Stability of polymeric Pt-cyanoximate 5 in the presence of DMSO.

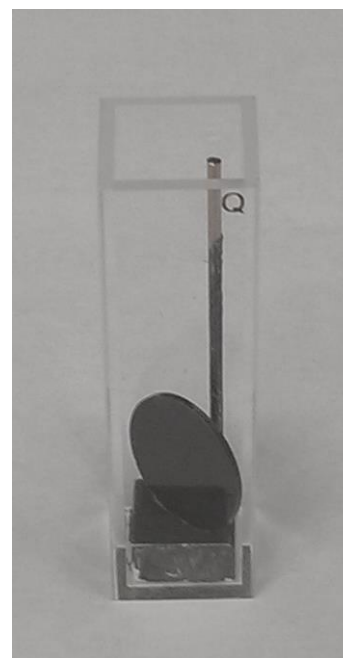
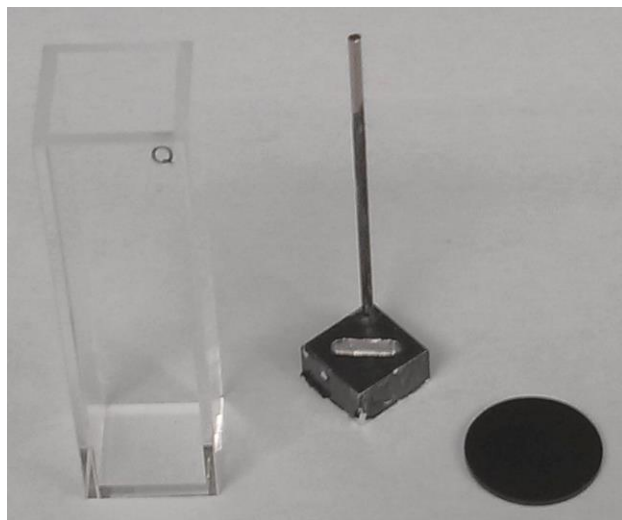
Time changes in UV-visible spectra of polymeric dark-green $[\text{Pt}(\text{DECO})_2]_n$ upon addition of DMSO. **A** – monitoring within 1 hr after addition of donor solvent; **B** – separate spectra within first 5-10 minutes showing quick decrease in 1D polymer content in the system.

**A****B**

5 Hardware for spectroscopy measurements

5.4 Tablet / pellet holder for spectroscopy measurements

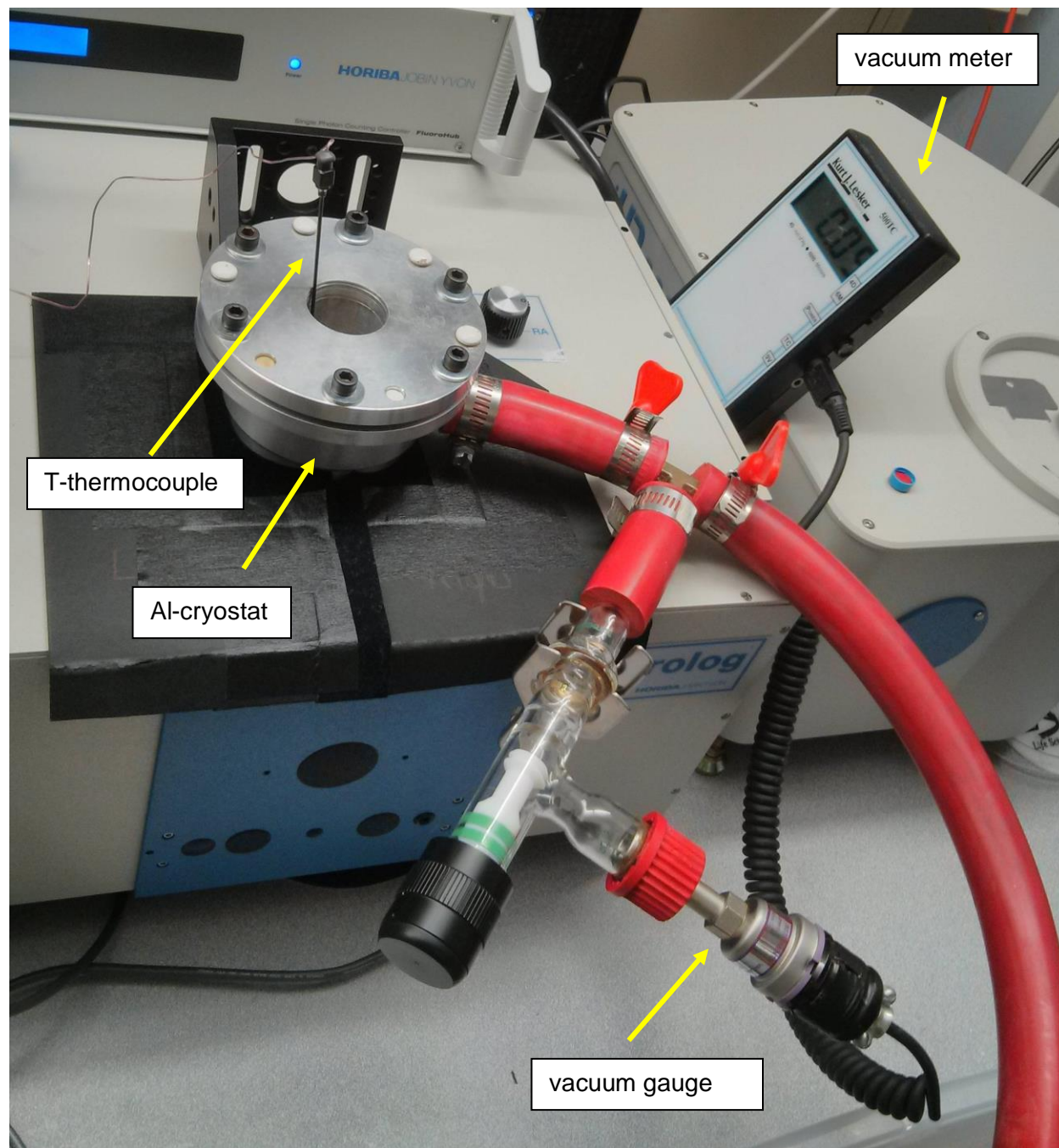
Top photograph shows 13 mm die/anvil hardened steel set used for pressing KBr pellets containing 5% (by weight) of studied compounds. Left photograph below shows individual pieces, such as 1 cm quartz cuvette, blackened Al-pellet holder with 1/16" width for the pellet, while the right photo displays complete assembly prior to its placement into the cuvette compartment of the spectrofluorimeter.



Other ionic solids transparent in the IR-region of electromagnetic spectrum were tested as inert matrices: CsI, CaF₂, NaF, LiF. However, KBr proved to be the best matrix.

5.5 Variable temperature photoluminescence measurements instrument design

Custom made liquid N₂ or hot water/oil filled cryostat for the PL measurements of solid samples of synthesized compounds.



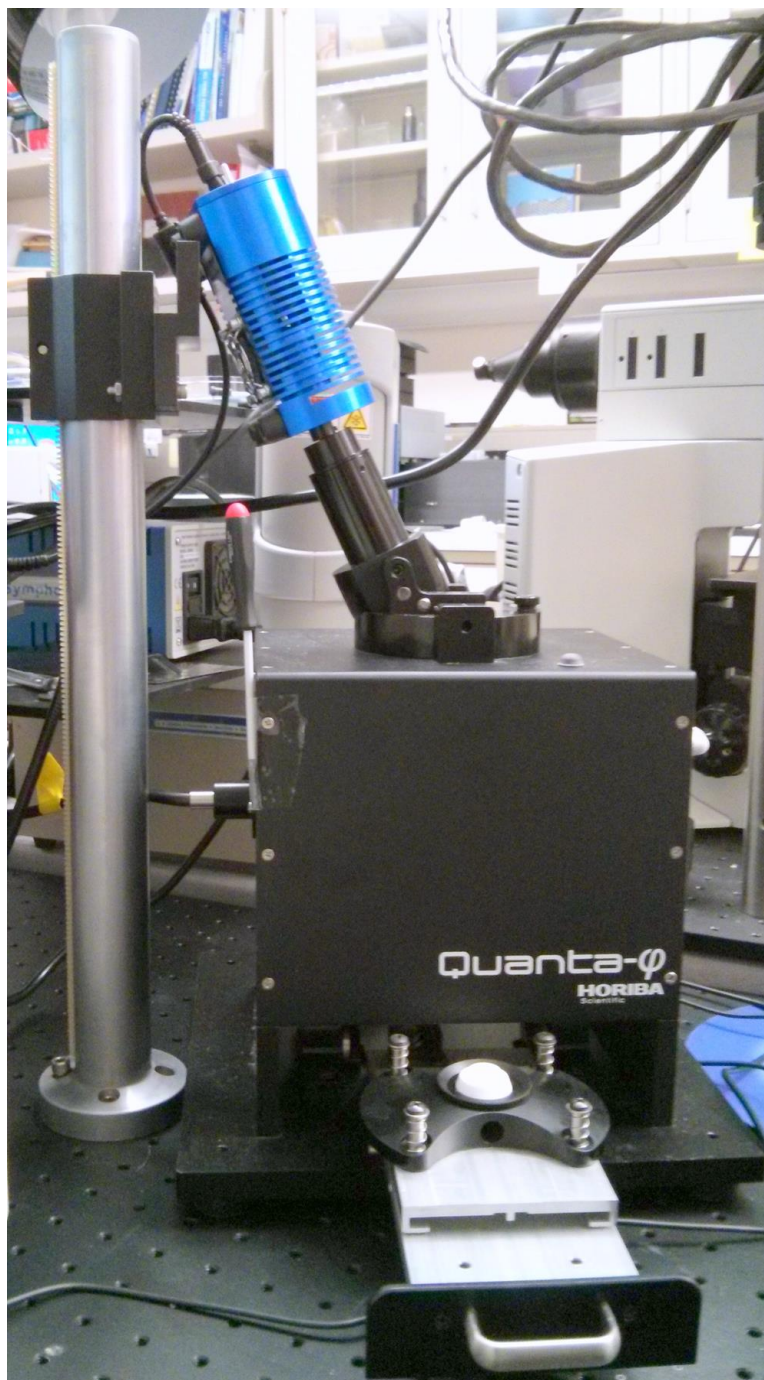
5.6 *Handling of samples for variable temperature photoluminescence measurements.*

Handling of samples of 1D polymeric $[\text{Pt}(\text{DECO})_2]_n$ (**5**) for solid state photoluminescence measurements: **A** – attachment of a fine powder to the surface of cold finger covered with double-sided $\frac{1}{2}$ " Scotch tape; **B** – KBr pellet containing ~5% of the complex adhered to cold finger.



5.7 *Solid state absorption spectra of tablets*

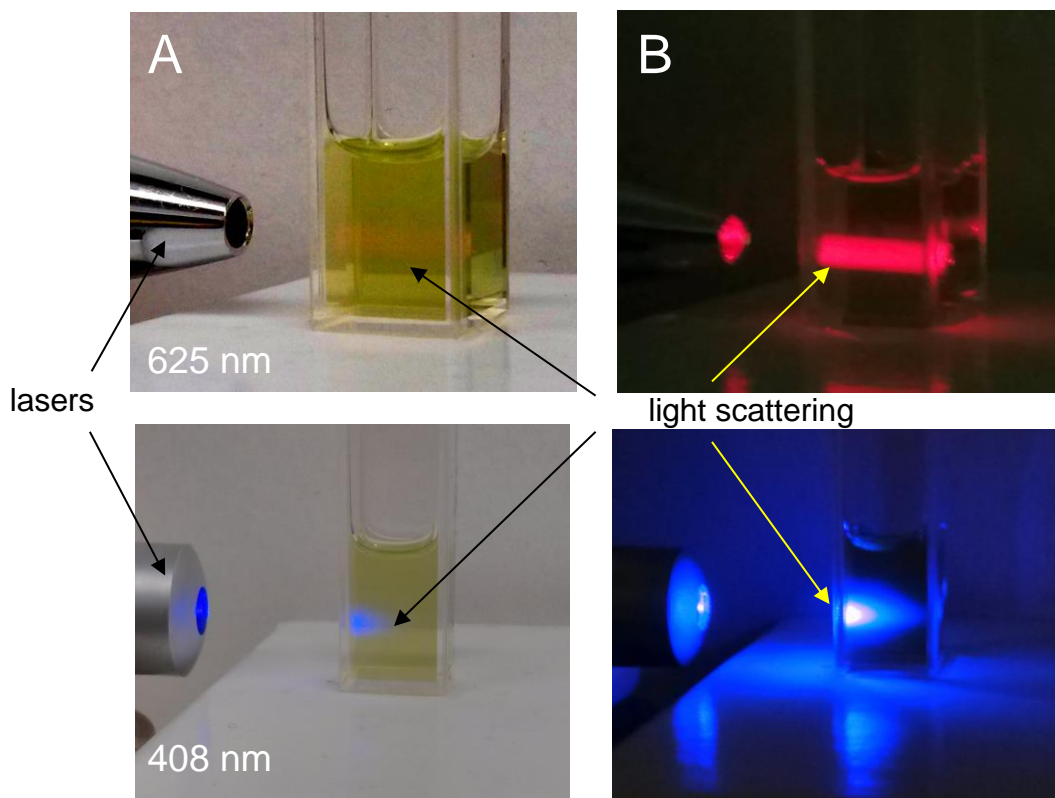
Solid state absorption spectra recorded for studied compounds in pressed with KBr (95%) pellets using an integrating sphere setup shown below. The spectra were normalized to light intensity and referenced to spectrum of pure KBr.



6 Optical and spectroscopic properties of the complexes

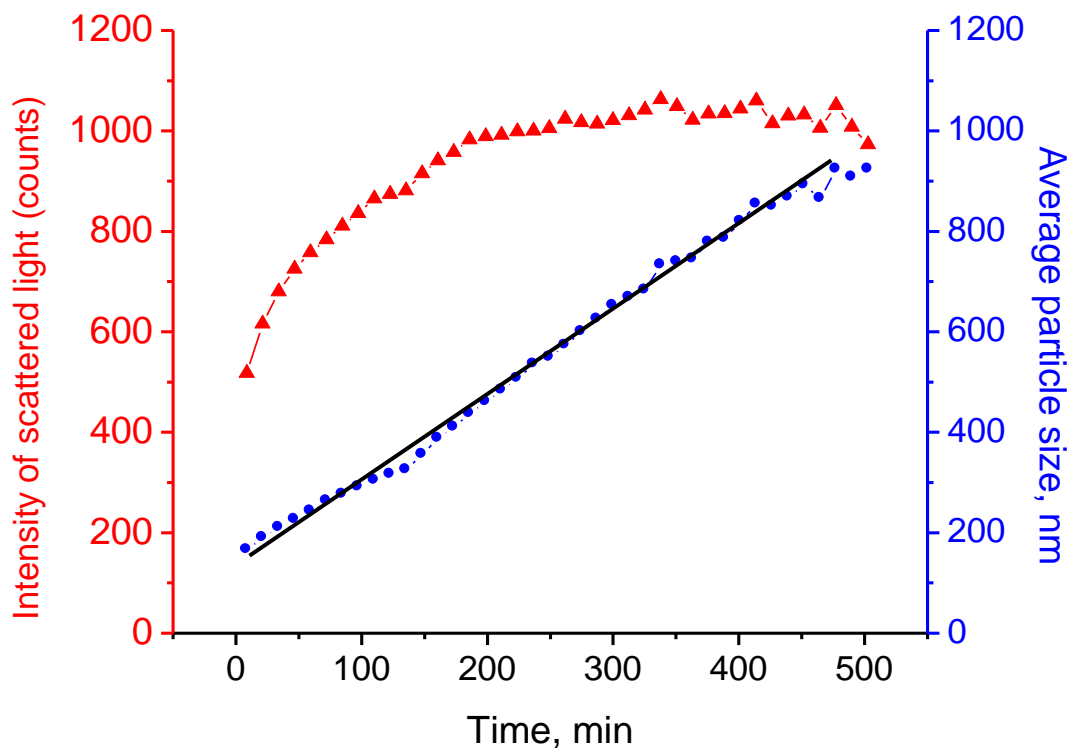
6.1 Scattering properties of polymeric Pt-cyanoximate 5

The Tindal effect in solutions of green Pt-cyanoximate **5**: light scattering from spontaneously self-assembled, aggregated nano-size particles of 1D solids of green $[\text{Pt}(\text{DECO})_2]_n$ in EtOH at day light (**A**), and in dark (**B**). Lasers with two different wavelength were used.



6.2 Kinetics of the particles size growth in solution of dark-green 1D polymeric complex 5.

Practically linear particles size growth (black line) for ~400 min time interval suggests an Ostwald ripening process of spontaneous aggregation of Pt(DECO)₂ complex **3** to “poker chip” stacks of [Pt(DECO)₂]_n (**5**) that have significant length. Black line well describes the linearity of the process, which then can be described as the Ostwald ripening.



6.3 Particles size measurements for the polymeric complex 5 in aqueous solutions of Na-decanoate micelles

Data of particles size measurements for the complex 5 dispersed in micelles formed in aqueous solutions of Na-decanoate, $C_{10}H_{21}COONa$ at $+23^{\circ}C$.

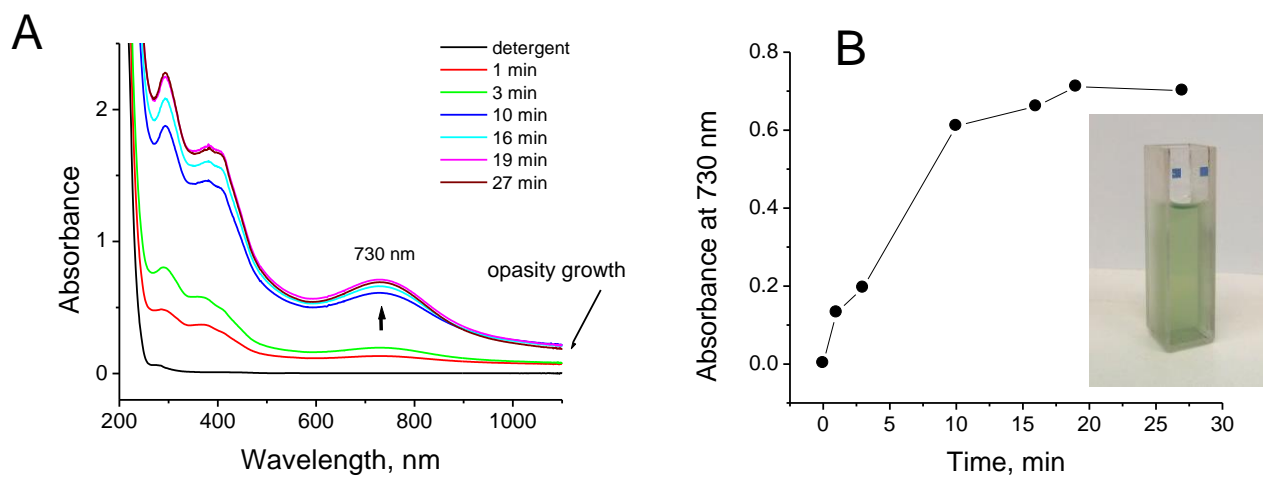


All Fields DLS Report

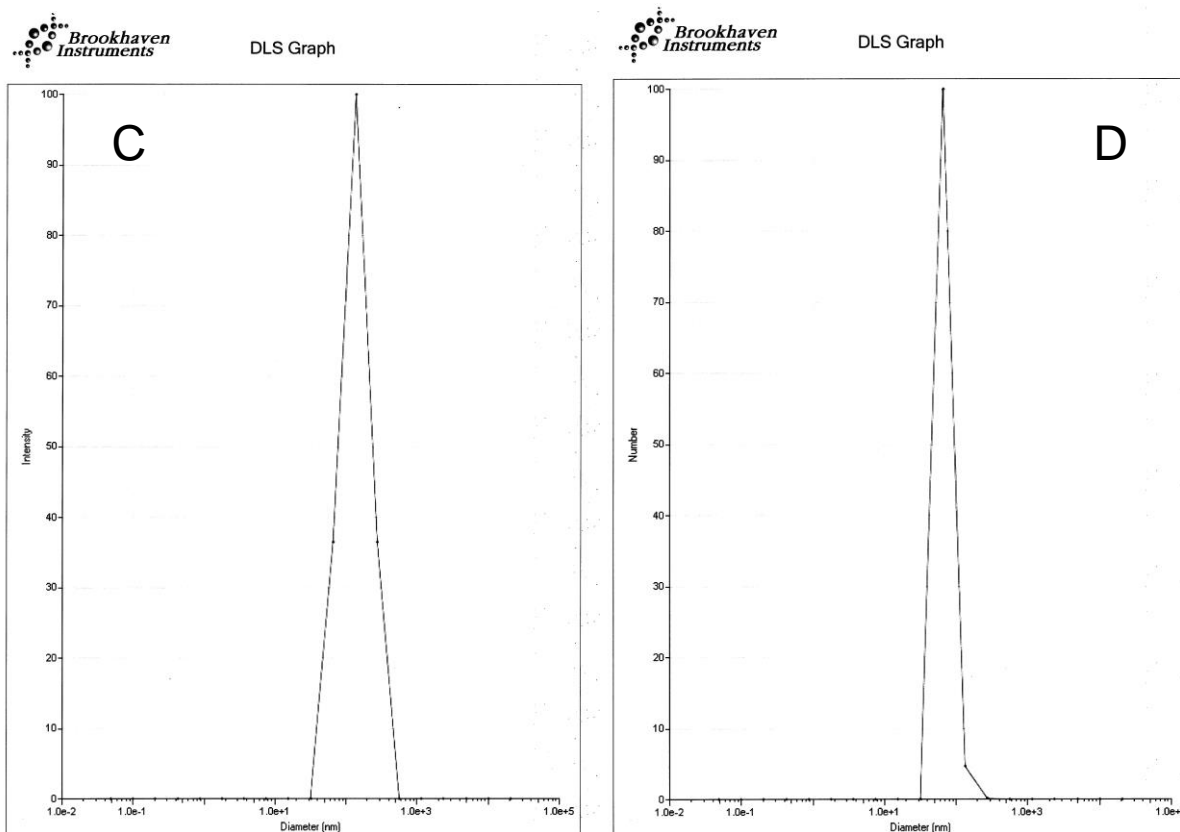
Sample		Results		Advanced ID	
Type:	DLS	Eff. Diam. (nm):	147.37	Project ID:	
Sample ID:	Pt(DECO)2-	Polydispersity:	0.198	Group ID:	NC
Operator ID:	Unknown Op	MHS Mol. Weight		Batch Number:	1
SOP ID:	NG Pt[DECO	MHS Parameters (K, a):	7.89E-05, -0.43	Rev #:	0
Start Date/Time:	10/27/201	MHS Molecular Weight (g/mol):	7.047e+07	Revision Date/Time:	
Imported Run #:	1	Measurement Conditions			
Measurement Sequence Start Date/Time:	10/27/201	Count Rate (kcps):	516.5	Dust Filter:	<input checked="" type="checkbox"/>
Notes:	Pt[DECO]2 G	Duration (hh:mm:ss):	00:01:40	Dust Cutoff:	30.00
Liquid		Baseline Index:	9.4	Normalization:	Autoslope
Liquid:	Water	Data Retained (%):	100.00	Cell Description:	BI-SCP
Temperature (°C):	25.00	Size Distribution			
Viscosity (cP):	0.8900	Particle Refractive Index, Real:	1.59	Particle Refractive Index, Imaginary:	0.00
Refractive Index:	1.3310	Mean Diam. By Intensity:	148.55	Variance By Intensity:	0.22
Scattering Angle (°):	90.00	Mean Diam. By Volume:	92.56	Variance By Volume:	0.28
pH:		Mean Diam. By Number:	68.15	Variance By Number:	0.05
Lognormal		Titration		Multimodal Size Distribution:	
Diam. 10 (nm):	85.42	pH Titration:	<input type="checkbox"/>		
Diam. 50 (nm):	147.37	Additive Titration:	<input type="checkbox"/>		
Diam. 90 (nm):	254.25	Additive Titration Volume Added (µL):			
Lognormal GSD:	1.53	Temperature Automation:	<input type="checkbox"/>		
Lognormal Mean Diam. (nm):	161.33	Concentration:			
Lognormal Median Diam. (nm):	147.37				

Results clearly indicate formation of mono-dispersed by size micelles of ~68 nm diameter. They could incorporate up to 210 stacked into 1D polymer $Pt(DECO)_2$ molecules as judged by Pt---Pt distance of 3.121 Å in a red $[Pt(DECO)_2]_2$ dimer 4 which is considered as a polymer building block (Figure 2 in the main text). These results are consistent with shown above in S37 data.

A – Changes in the UV-visible spectra of Na-decanoate (detergent) upon addition of dark-green complex 5; **B** – time profile of micelles stability with an inset showing their actual appearance;



C – distribution of particles size by intensity, and **D** – by the number.



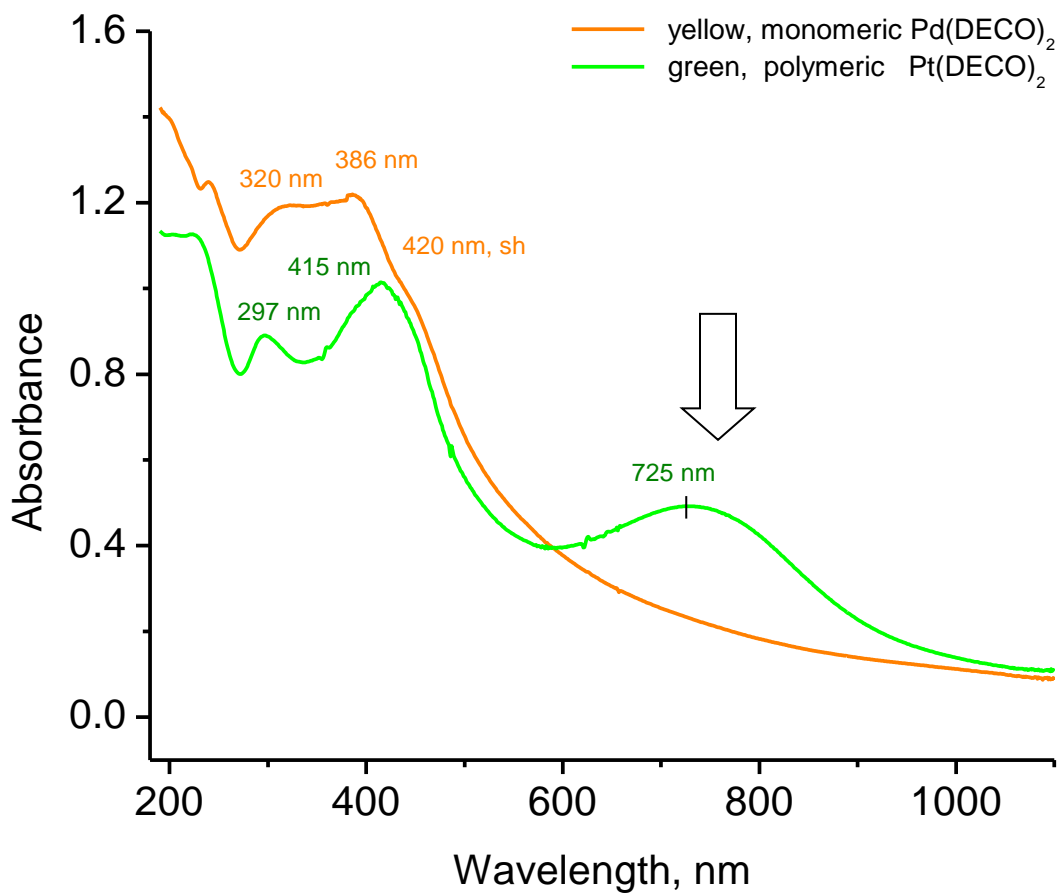
6.4 UV-Vis spectroscopy measurements (summary)

Data of UV-Vis spectroscopy measurements for HDECO (**1**), its anion, DECO⁻ (**2**, as NH₄⁺ salt), and yellow monomeric Pd(DECO)₂ (**6**) and Pt(DECO)₂ (**3**).

Compound	Solvent	C (mM)	λ_{\max} (nm)	ϵ (M ⁻¹ · cm ⁻¹)	Comment
Organic ligands:					
1	H ₂ O	n/a	n/a	n/a	insoluble in water
2	H ₂ O	2.92	375	62	$n \rightarrow \pi^*$
1	CH ₃ OH	1.58	226	10330	$\pi \rightarrow \pi^*$
2	CH ₃ OH	1.58	394	73	$n \rightarrow \pi^*$
1	C ₂ H ₅ OH	1.52	228	9200	$\pi \rightarrow \pi^*$
2	C ₂ H ₅ OH	1.52	~387	(shoulder)	$n \rightarrow \pi^*$
1	<i>n</i> -C ₃ H ₇ OH	2.67	229	3625	$\pi \rightarrow \pi^*$
2	<i>n</i> -C ₃ H ₇ OH	2.67	285 393	3940 28	$\pi \rightarrow \pi^*$ $n \rightarrow \pi^*$
2	DMF	1.53	472	47	visible region only! UV not transparent
2	DMSO	4.01	469	60	visible region only! UV not transparent
Metal complexes:					
6	DMSO	1.0	311 368	18120 16400	$\pi \rightarrow \pi^*$ $\pi \rightarrow \pi^*$
3	DMSO	1.0	315 381	12900 9550	$\pi \rightarrow \pi^*$ $\pi \rightarrow \pi^*$

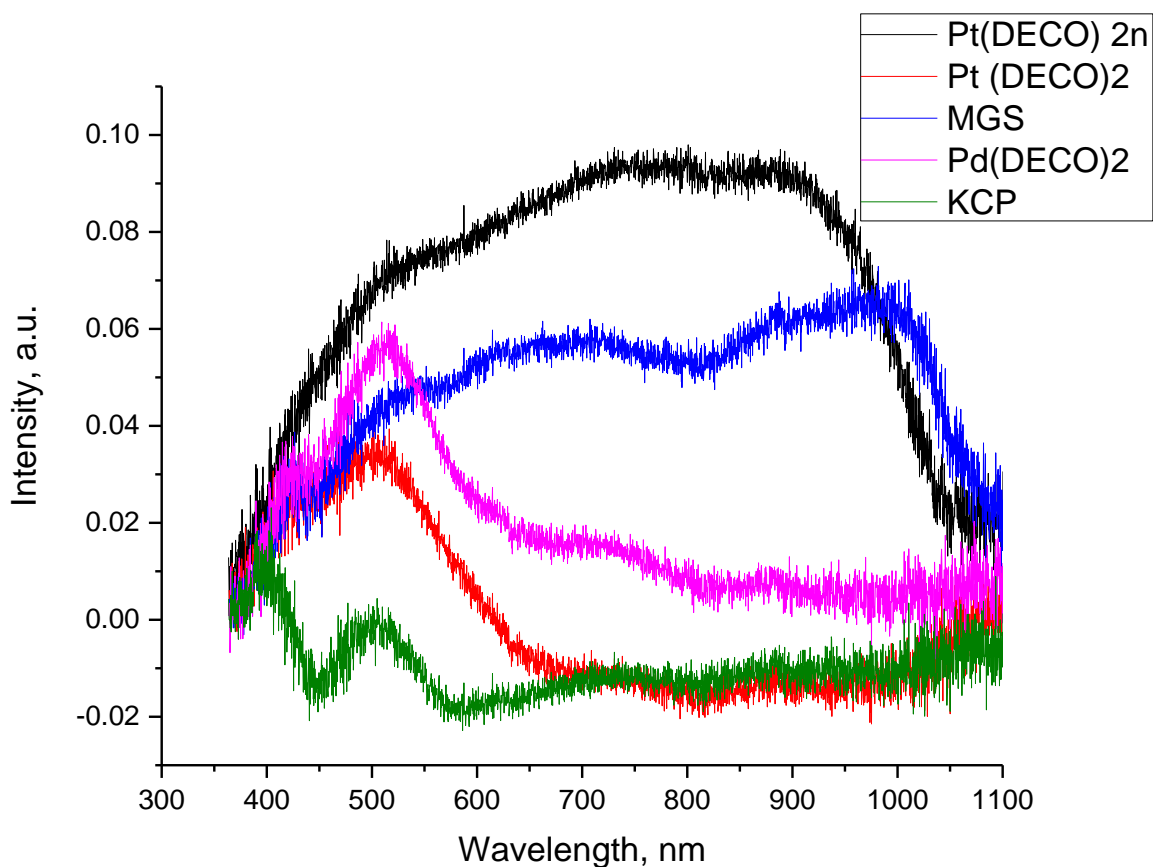
6.5 Solid state absorption spectra recorded as fine suspensions in mineral oil

Solid state absorption spectra (recorded as fine suspensions in mineral oil) of 1D polymeric, dark-green $[\text{Pt}(\text{DECO})_2]_n$ (**5**) and yellow monomeric $\text{Pd}(\text{DECO})_2$ (**6**); $T=+20^\circ\text{C}$. Color coded numbers indicate maxima in both spectra, while an arrow shows wavelength (785 nm) used for the excitation during recording solid samples photoluminescence.



6.6 Solid state absorption spectra of tablets

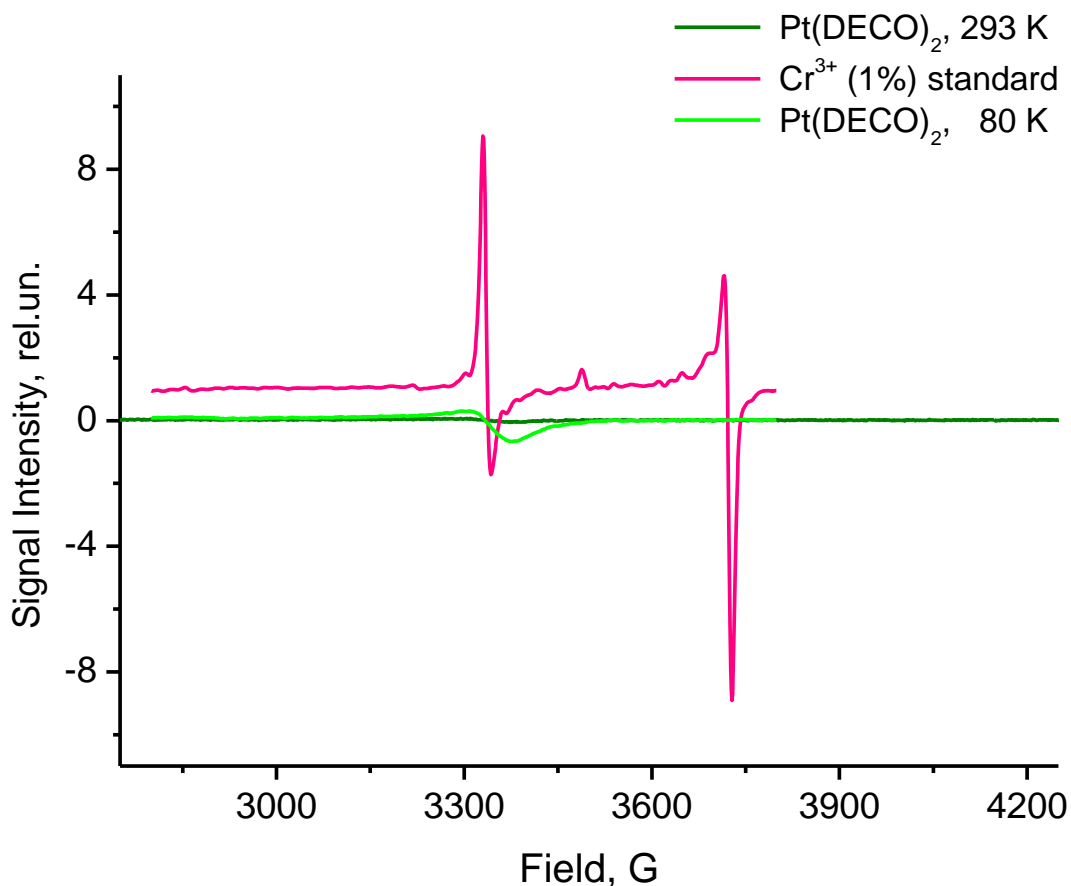
Solid state absorption spectra recorded in KBr tablets in an integrating sphere setup. Spectra normalized to light intensity and referenced to the spectrum of pure KBr. Black trace - 1D Pt polymeric complex **5**; red - Pt monomeric complex **3**, magenta - Pd monomeric complex **6**, while blue and green traces define spectra of a control model 1D solids.



6.7 EPR spectra of solid samples of 1D polymer 5

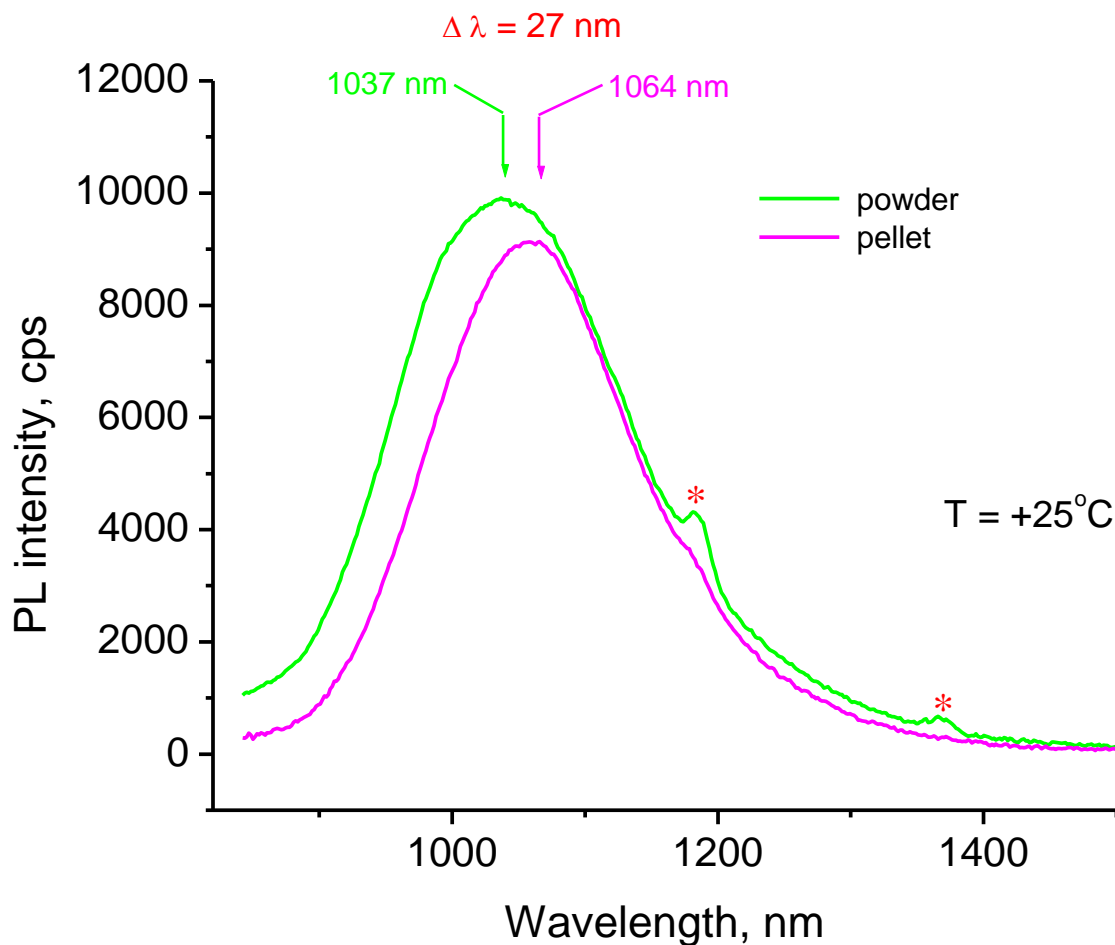
EPR spectra of powdery samples of studied $[\text{Pt}(\text{DECO})_2]_n$ dark-green polymeric complex **5** at 293 and 80 K (green traces) and sensitivity standard containing 1% of Cr(III) in $\text{Al}_2(\text{SO}_4)_3$ (pink trace). Parameters: center field at 3300 G with sweep width 1000 G; time constant 160 ms, sum of five repetitions.

Data evidenced absence of Pt(III) species which adopt low-spin d^7 configuration (Kramers' doublet) in square-planar environment which should be easily observed.



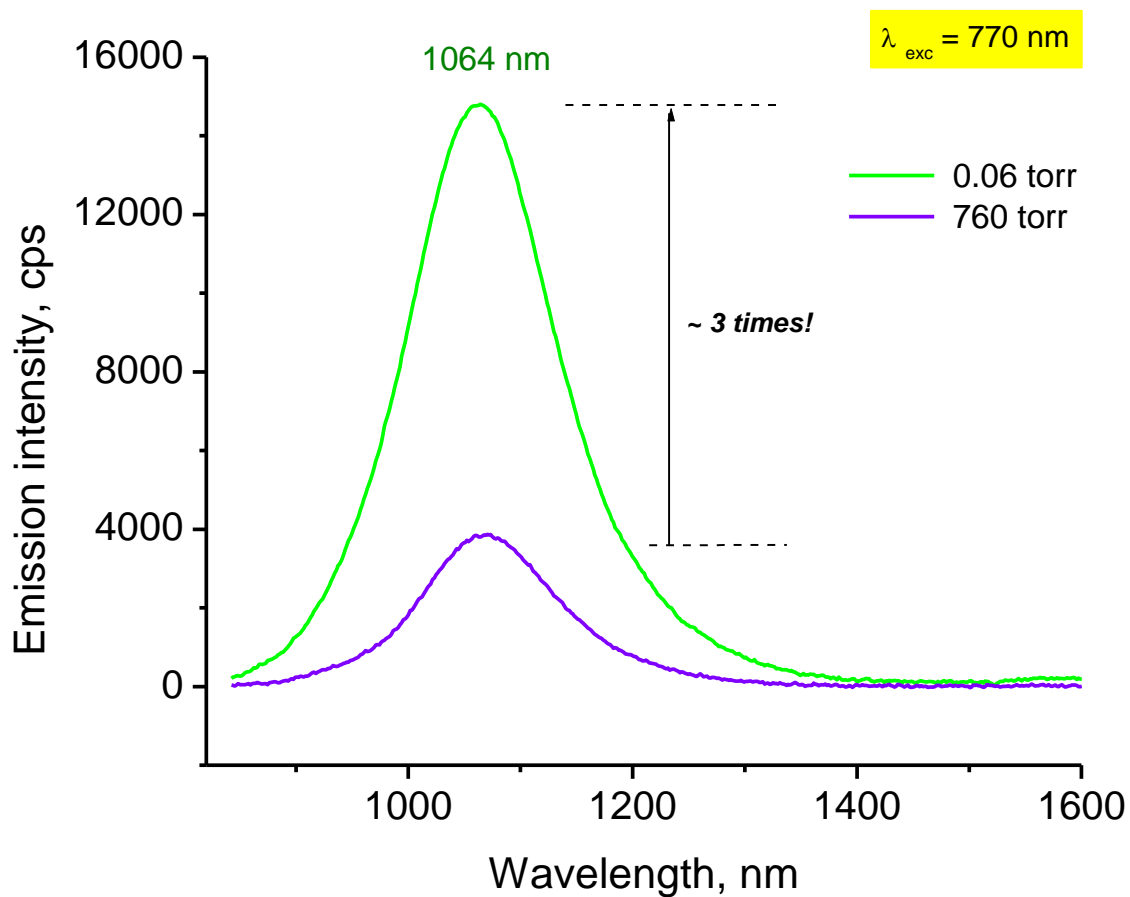
6.8 Photoluminescence of powder samples

Photoluminescence of 1D polymeric, dark-green $[\text{Pt}(\text{DECO})_2]_n$ (**5**) from pure powder and from the pellet in KBr (5% by weight). Powder of the complex was spread over the double-sided Scotch tape (1/2" width) attached to the cold finger of the cryostat (see **S33** above for details). Asterisks indicate instrumental artifacts.



6.9 Effect of air on photoluminescence of complex 5.

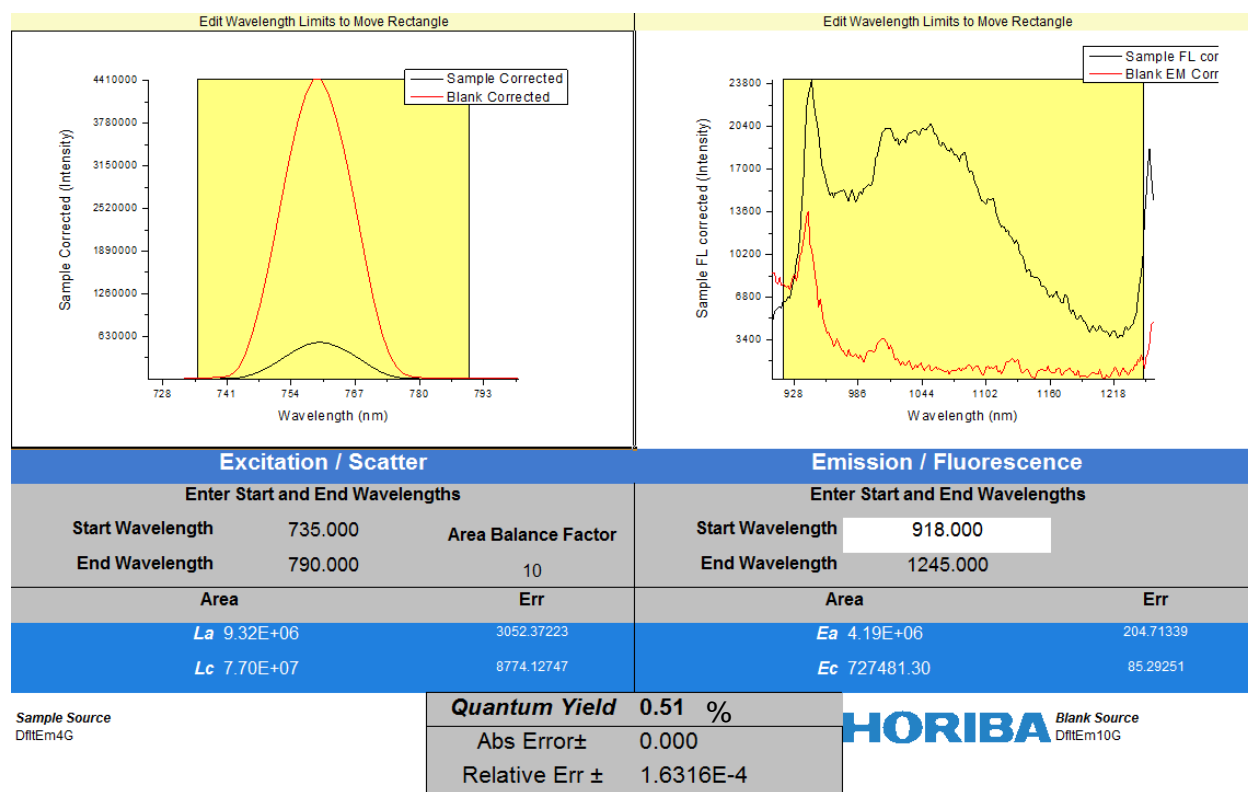
Emission spectra of $[\text{Pt}(\text{DECO})_2]_n$ dark-green sample, **5**, as 5% pellet in KBr, in vacuum and on air. Clearly shown dramatic increase in PL intensity upon removal of atmospheric O_2 which suggests phosphorescence origin of the observed emission. $T=+25^\circ\text{C}$, CCD detector; both emission and excitation slits are 14.7 nm, with $\lambda_{\text{exc}}=770$ nm and 20 s exposition time.



6.10 Absolute quantum yield determination

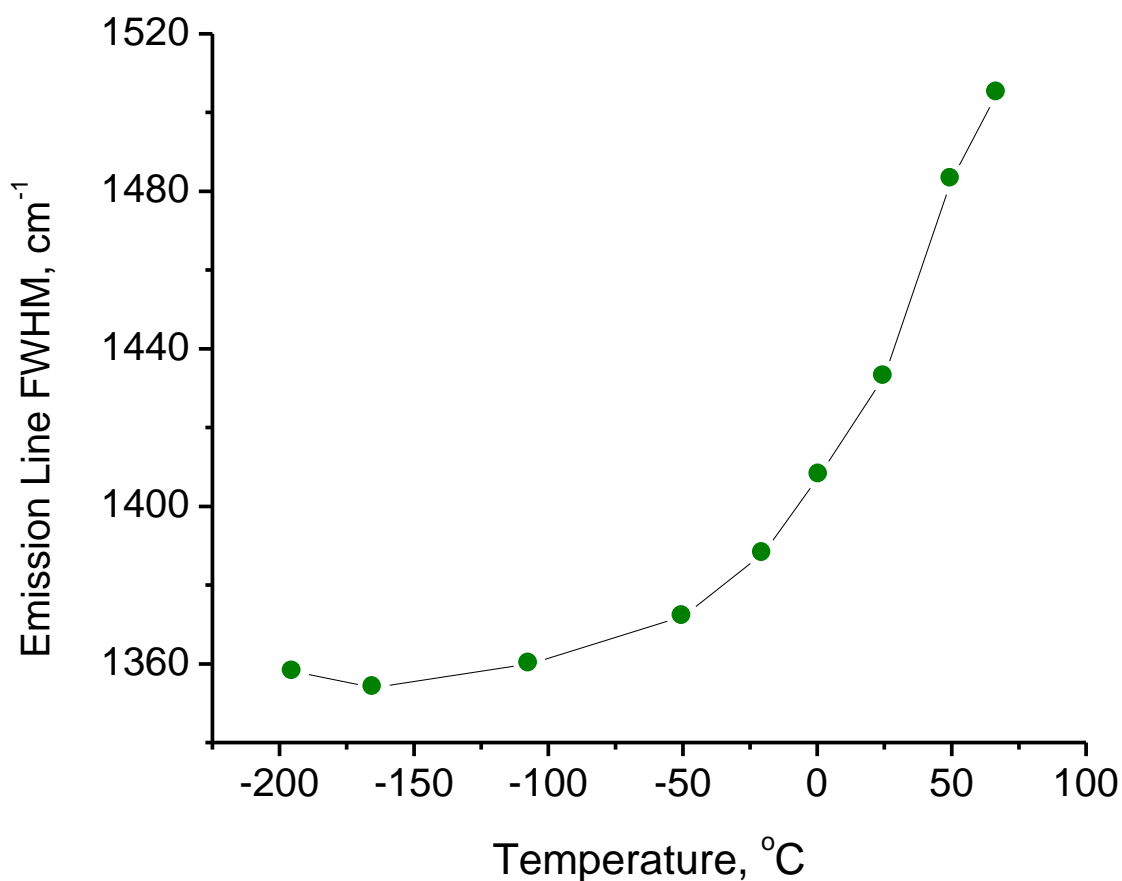
An assessment of the quantum yield (QY) of the photoemission from KBr pellet with dark-green 1D polymeric Pt-cyanoximate **5** (at 5 weight % concentration) using absolute total reflectance from the sample. The ratio of intensities of reflected light at excitation wavelength vs intensity of emitted light allows determination of QY for solid samples in the absence of standard calibration materials or compounds. Indeed, contrary to solution samples for solids there are no accepted and trustful compounds with calibrated QY since it depends heavily on the sample history (such as: method of sample preparation, its density, thickness and surface area).

Ex 770 nm; em. 820-1200 nm, QY = 0.51%



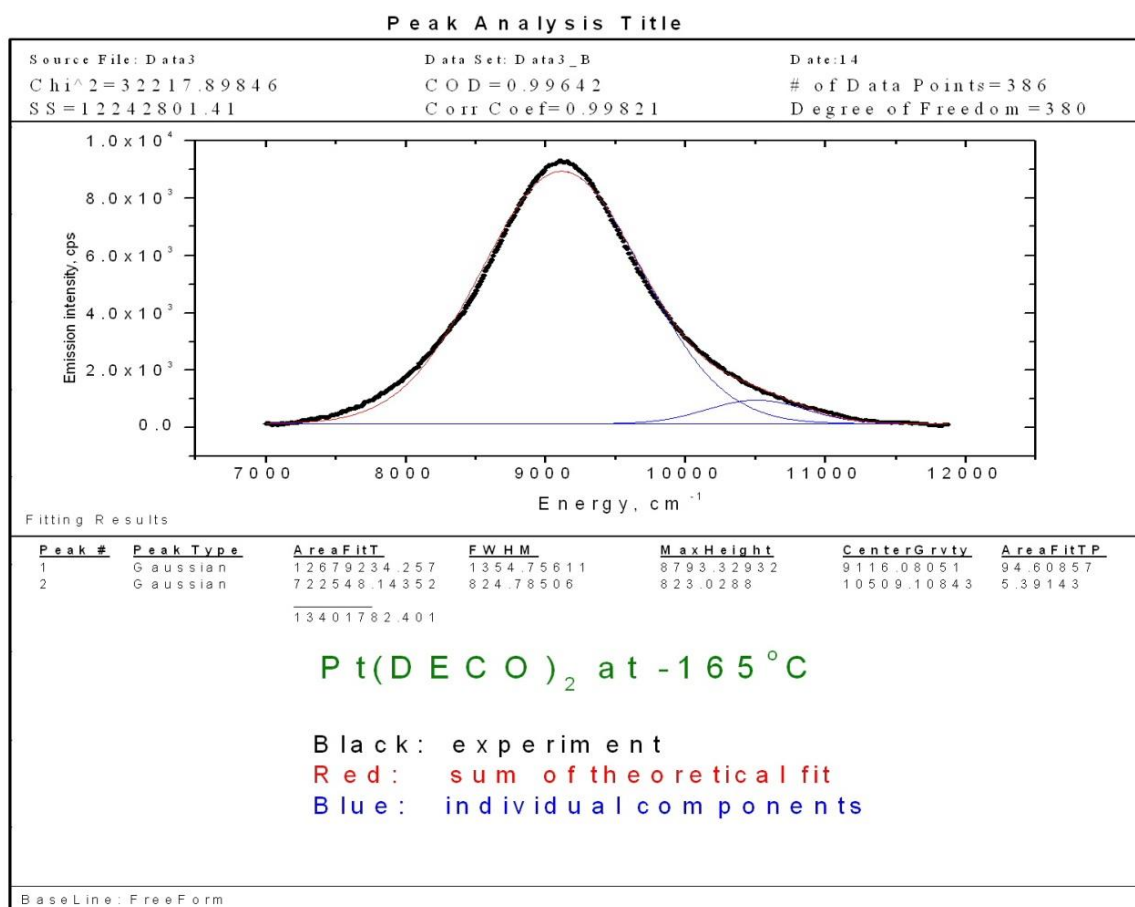
6.11 Temperature dependence of the emission line width for solid sample of dark-green polymeric complex 5

Plot of the line NIR emission main line width from $[\text{Pt}(\text{DECO})_2]_n$ sample temperature. A significant decrease in the width is indicative of the electron relaxation time increase upon temperature descend which is consistent with its more localized behavior. This temperature profile is typical of other 1D solids such as KCP and red dimeric PtLX_2 (L = dipy, phen; X = Cl, Br, CN).

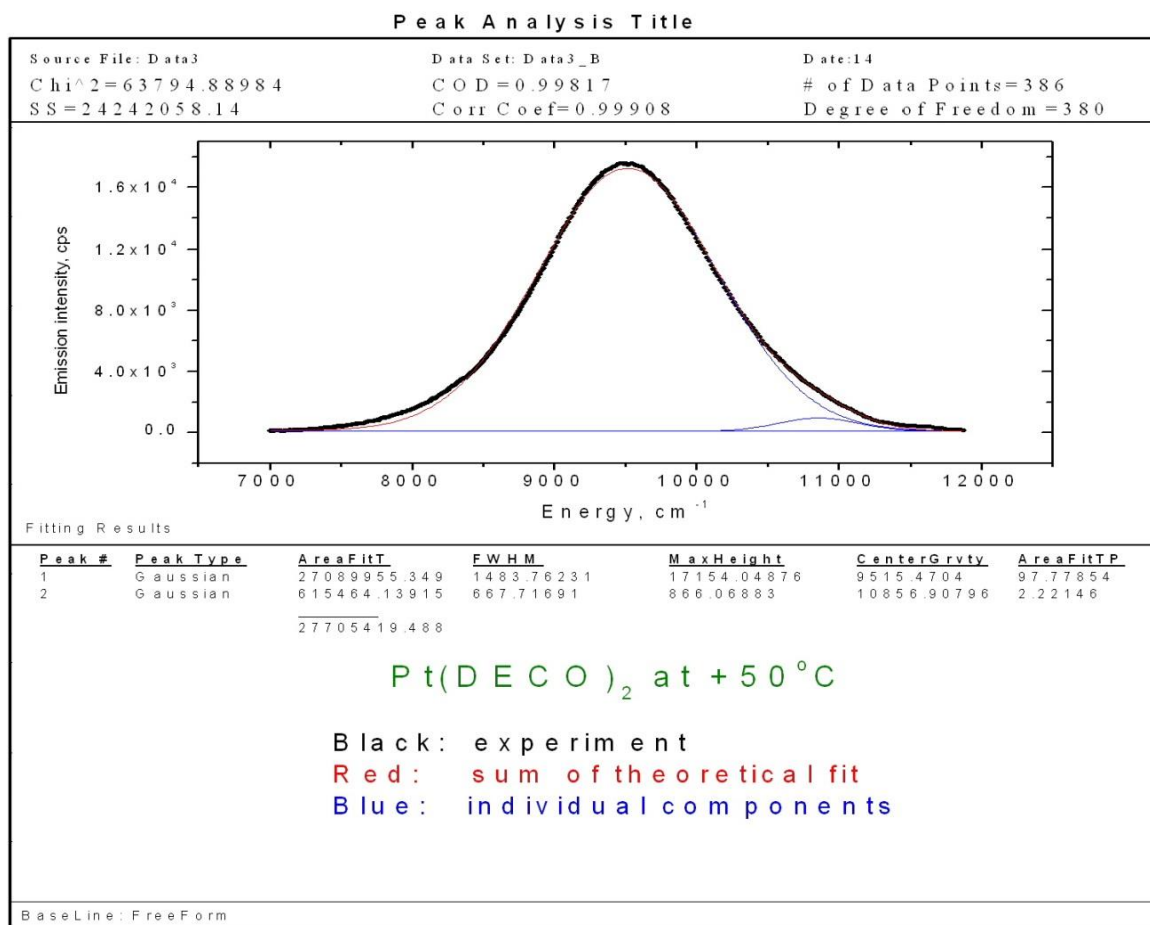


6.12 The emission line shape analysis for solid sample of complex 5 (in KBr pellet; at 5% concentration) at -165°C .

Line shape analysis of the NIR emission from $[\text{Pt}(\text{DECO})_2]_n$ at 770 nm excitation wavelength; detector - CCD camera. The best fit was obtained when two Gaussian-type lines were used indicating a two component emission from the sample.

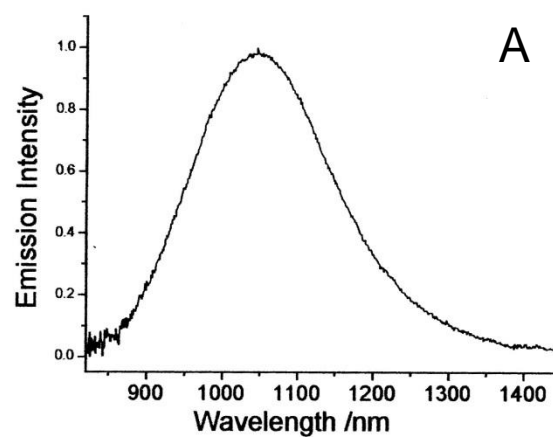
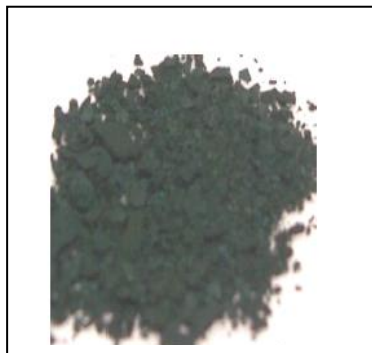


6.13 The emission line shape analysis for complex 5 at +50°C.

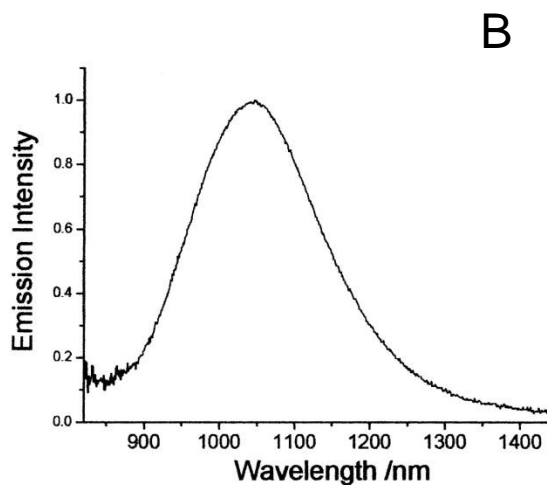
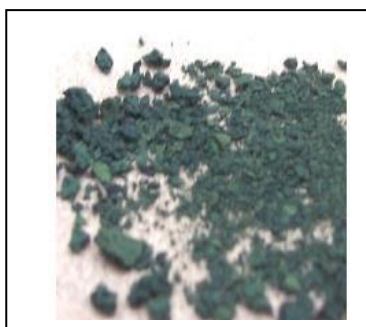


6.14 The emission spectra of other two dark-green polymeric Pt-cyanoximates.

Preliminary NIR spectra of solid samples of dark-green polymeric forms of [cis-Pt(PiPCO)₂]_n at (A), and [cis-Pt(MCO)₂]_n (B) at 296 K. Both spectra recorded with the help of Prof. V.Yum.



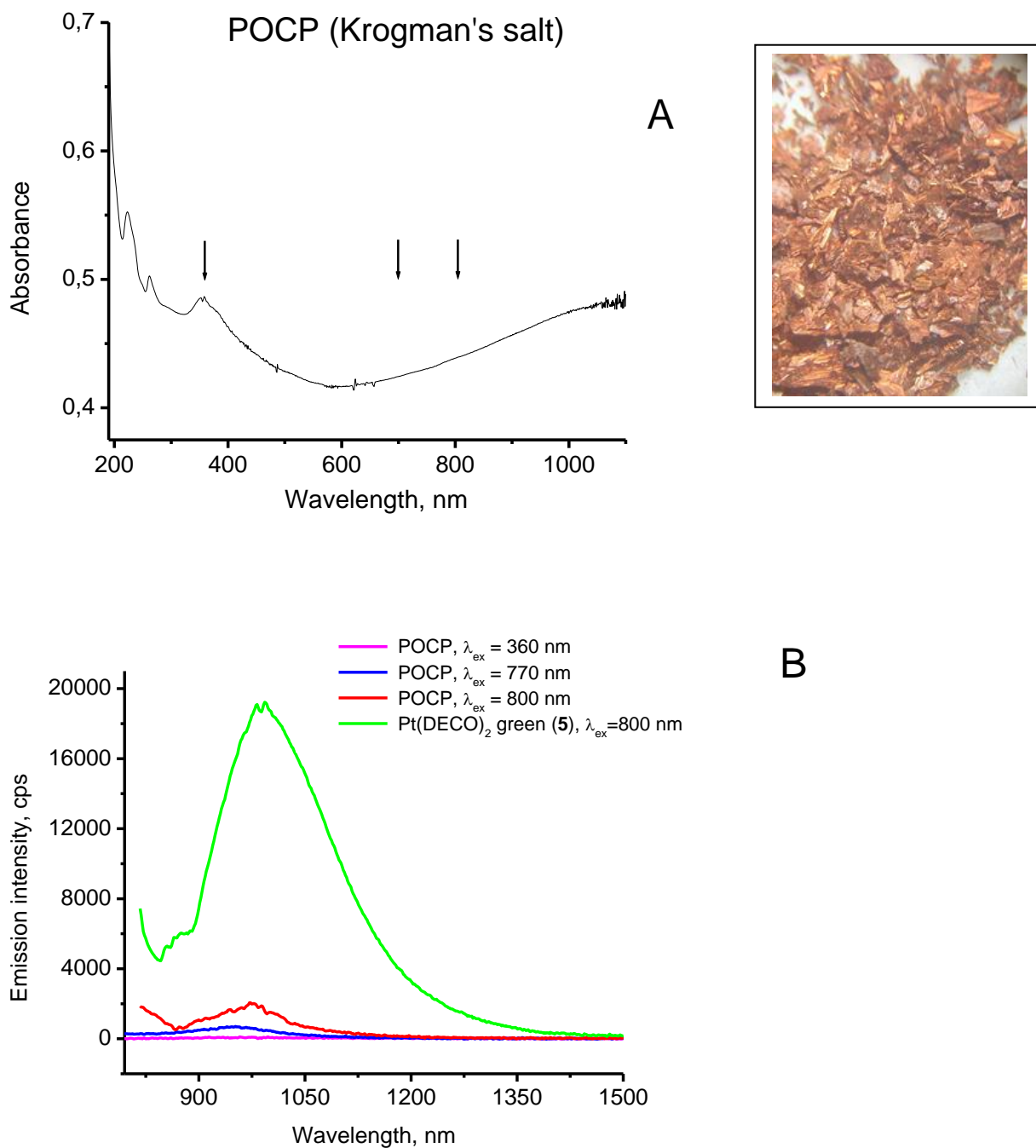
$\lambda_{\max} \sim 1047$ nm



$\lambda_{\max} \sim 1045$ nm

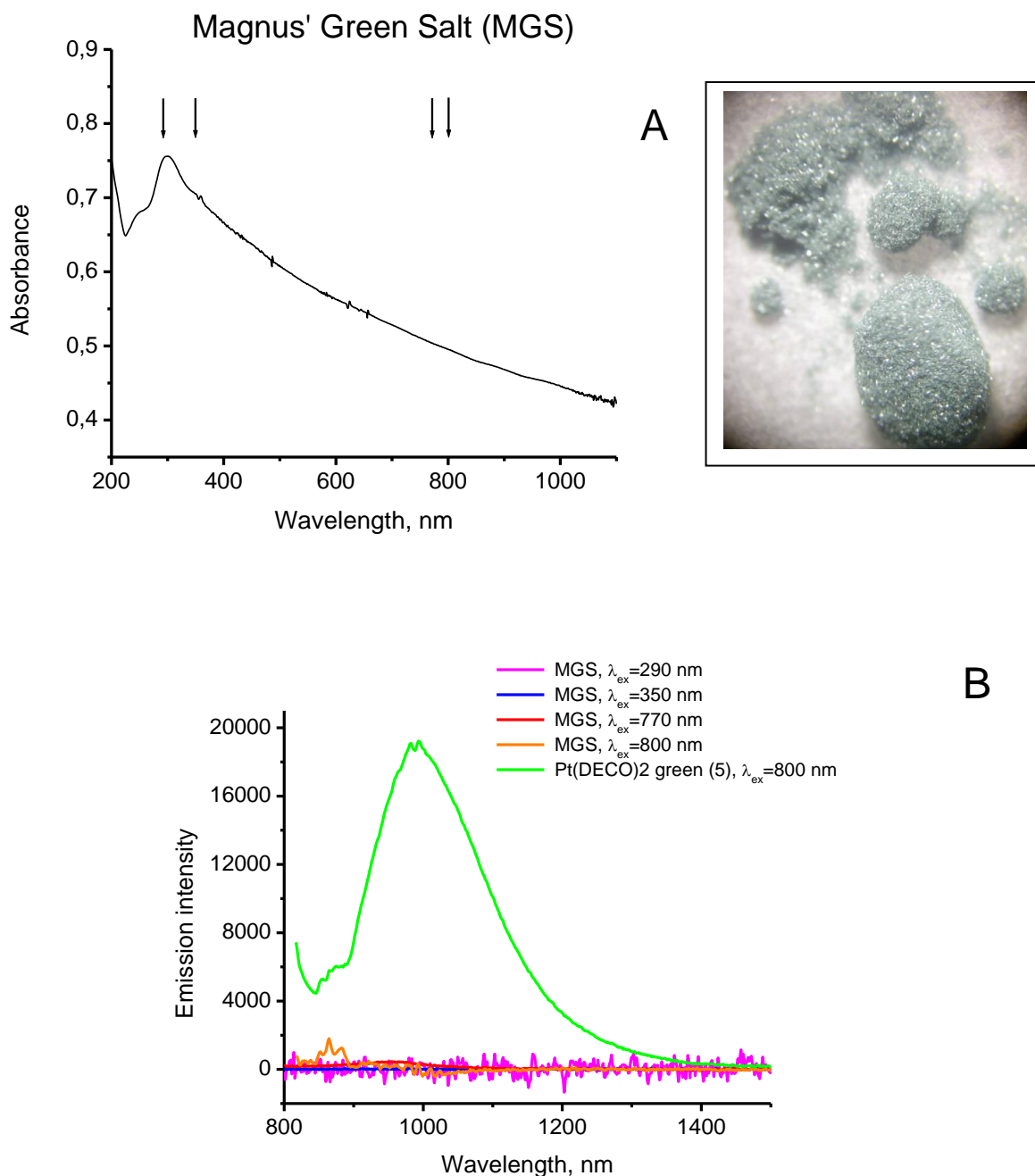
6.15 The absorption (A) and emission spectra (B) of the Krogman's salt (POCP) used as control mixed valence compound with known structure.

Spectrum A recorded as fine suspension in mineral oil at room temperature. Arrows indicate three wavelengths at which emission spectra were measured. An inset shows complex's actual appearance. Spectrum of presented in this paper polymeric complex **5** is shown for comparison.



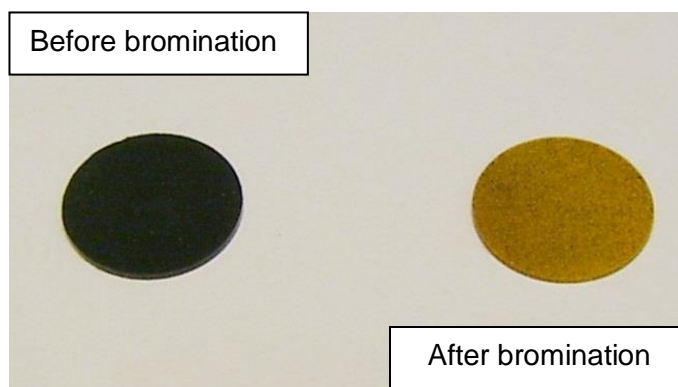
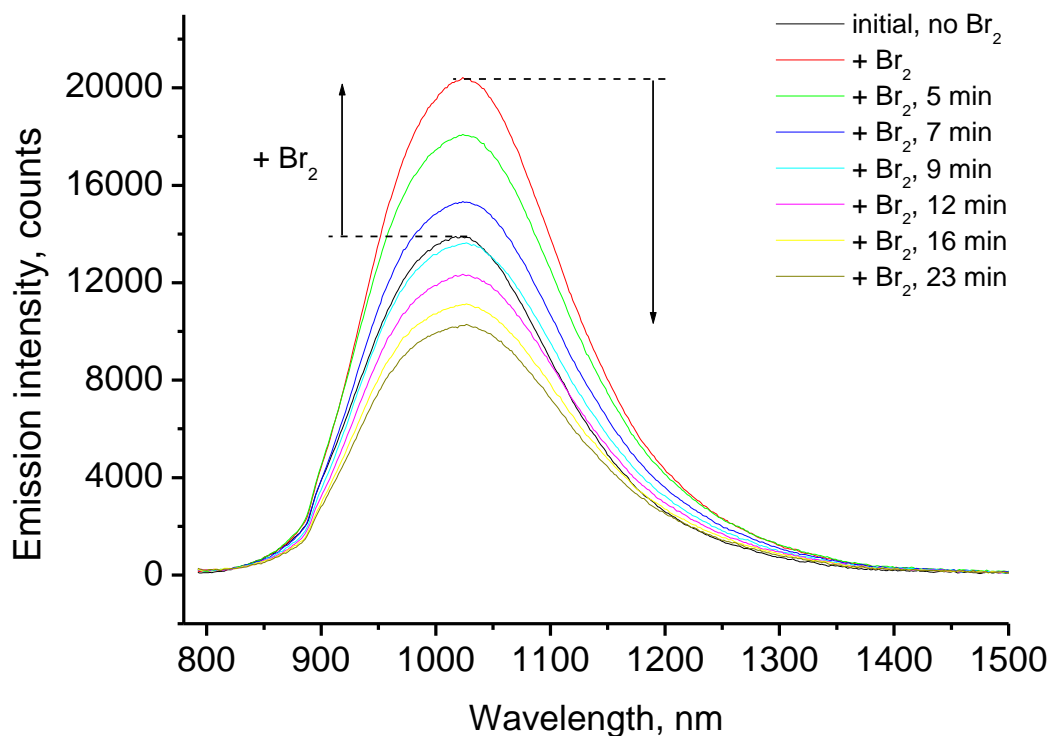
6.16 *The absorption (A) and emission spectra (B) of the Magnus' Green Salt (MGS) used as control complex with 1D structure.*

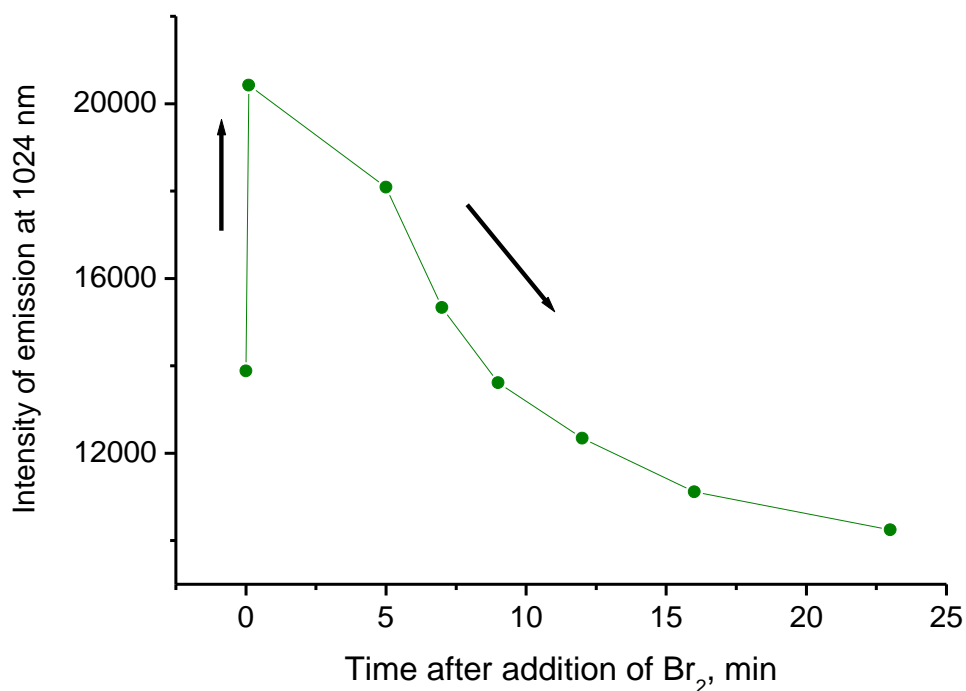
Spectrum **A** recorded as fine suspension in mineral oil at room temperature. Arrows indicate three wavelengths at which emission spectra were measured. An inset shows complex's actual appearance. Spectrum of presented in this paper polymeric complex **5** is shown for comparison.



6.17 Oxidation of 1D-polymeric complex 5 with elemental Br₂.

During first minute there was ~30% jump up in the emission intensity. After longer exposure pellet started deteriorating due to the complex/ligand bromination. It should be noted that the oxidation of bivalent platinum in K₂[Pt(CN)₄] (classic KCP) with Br₂ leads only to ~32% of metal centers oxidized in thus formed Krogman's salt K₂[Pt(CN)₄] Br_{0.3} x 3H₂O (classic POCP, metallic conductor – see picture below). In our case roughly the same increase in the emission intensity also is due to partial oxidation of Pt(II) in Pt(DECO)₂ complex.



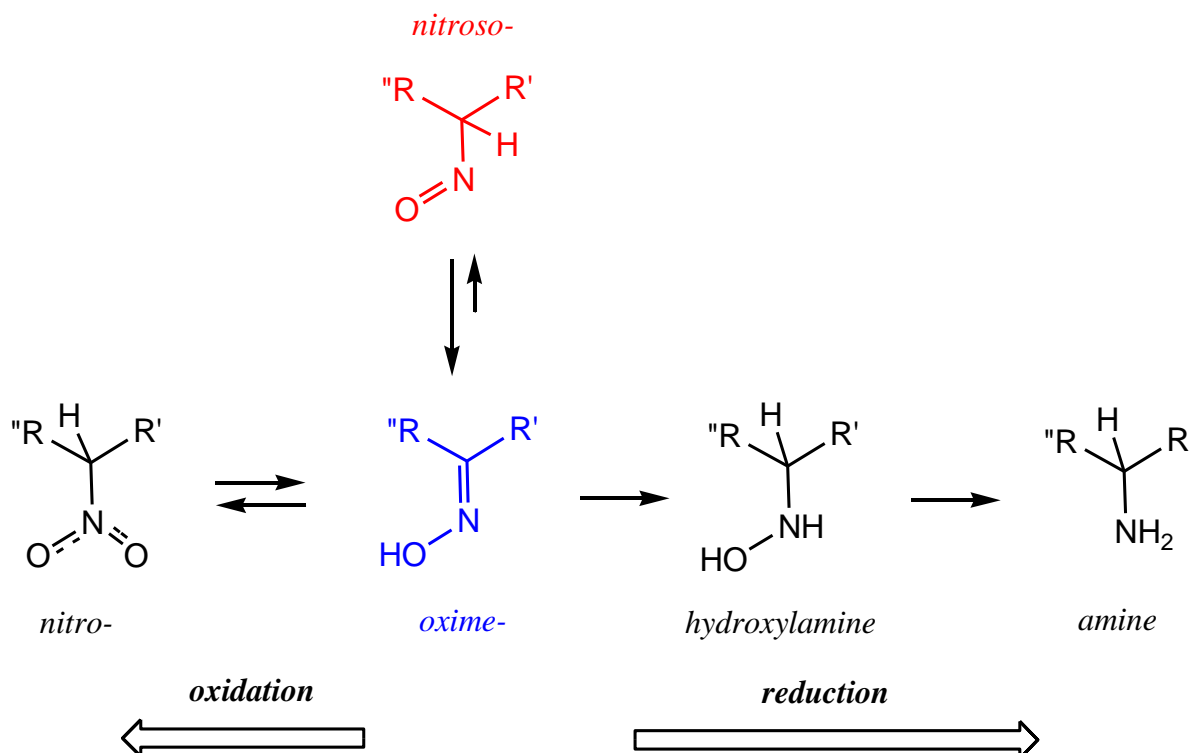


During first minute there was ~30% jump up in the emission intensity. After longer exposure pellet started deteriorating due to the complex/ligand bromination. It should be noted that the oxidation of bivalent platinum in $K_2[Pt(CN)_4]$ (classic KCP) with Br_2 leads only to ~32% of metal centers oxidized in thus formed Krogman's salt $K_2[Pt(CN)_4] Br_{0.3} \times 3H_2O$ (classic POCP, metallic conductor – see picture below). In our case roughly the same increase in the emission intensity also is due to partial oxidation of Pt(II) in $[Pt(DEC O)_2]_n$ complex **5**.

Fast and significant increase in the emission intensity upon sample exposure to oxidizer evidences origin of the NIR emission from mixed valence dark-green 1D polymer **5**. The initial complex contains small, non-stoichiometric amount of Pt(IV) centers that could appear in the sample due to the redox processes during synthesis involving oxidation of Pt(II) either: a) via air from oxygen, or b) by the cyanoxime. The first process seems unlikely due to similarity of UV-visible spectra during reaction monitoring at aerated and anaerobic conditions.

6.18 Redox flexibility of the nitroso/oxime compounds.

The relationship between different classes of NO/NH containing compounds:



The oxidation of oximes/nitroso compounds was known to be successfully carried out using KMnO_4 or $\text{K}_2\text{S}_2\text{O}_8$ by H. Köhler in the '70th. The reduction of oximes/nitroso compounds to amines using Na_2S or Zn chunks was discovered by N.N. Zinin and widely used in syntheses of anilines.